


Article

Thermal Comfort in Urban Open Green Spaces: A Parametric Optimization Study in China's Cold Region

Jiayi Lin ¹, Songlin Jiang ¹, Shuangyu Zhang ¹, Siyu Yang ¹, Wenli Ji ^{1,*}  and Weizhong Li ^{2,*}

¹ College of Landscape Architecture and Art, Northwest A&F University, Yangling, Xianyang 712100, China; 18729202177@163.com (J.L.); songlinjiang9@outlook.com (S.J.); 2020060553@nwafu.edu.cn (S.Z.); 15283891029@163.com (S.Y.)

² College of Forestry, Northwest A&F University, Yangling, Xianyang 712100, China

* Correspondence: jiwenli@nwsuaf.edu.cn (W.J.); liweizhong@nwsuaf.edu.cn (W.L.)

Abstract: In this study, typical open spaces were selected in the urban area of Lanzhou, China, with varying distances from the Yellow River and different plant configuration spaces. Then, the thermal perception of respondents was investigated through meteorological measurements, thermal comfort questionnaires, and parametric modeling. The findings indicate the following: (1) Wind speed decreases significantly as the distance from the Yellow River increases in the three open green spaces. (2) The cold lake effect of the Yellow River dominates the wind environment. (3) The closest site to the Yellow River exhibits the strongest correlation between wind speed and the respondents' thermal sensation. (4) There is a strong positive correlation between the model output and different spatial measurement values. (5) There is a certain discrepancy between the UTCI values and the actual measurements, but the fit is high and consistent with an R-squared value of 0.936. This study quantitatively evaluated the thermal comfort and perception in typical spaces and validated the reliability of parameterized modeling for such spaces, providing a reference basis for thermal environment planning in these spaces.

Keywords: open green space (OGS); thermal comfort; Universal Thermal Comfort Index (UTCI); ladybug tools; bioclimatic design; China's cold region



Citation: Lin, J.; Jiang, S.; Zhang, S.; Yang, S.; Ji, W.; Li, W. Thermal Comfort in Urban Open Green Spaces: A Parametric Optimization Study in China's Cold Region. *Buildings* **2023**, *13*, 2329. <https://doi.org/10.3390/buildings13092329>

Academic Editors: Ricardo M. S. F. Almeida and Vincenzo Costanzo

Received: 3 August 2023

Revised: 28 August 2023

Accepted: 6 September 2023

Published: 14 September 2023



Copyright: © 2023 by the authors. Licensee MDPI, Basel, Switzerland. This article is an open access article distributed under the terms and conditions of the Creative Commons Attribution (CC BY) license (<https://creativecommons.org/licenses/by/4.0/>).

1. Introduction

The global urbanization rate is rapidly increasing, and it is expected that by 2050, nearly 70% of the world's population will reside in urban areas, according to data from the United Nations (2018). There has been growing concern about the negative environmental impacts of urban areas, with the impact of urban microclimate on public health already being documented; however, people's attention to microclimate in river basin cities was low [1]. As the capital city of Gansu Province, Lanzhou is located in the upper reaches of the Yellow River and at the geometric center of China's continental territory, and it is the only city through which the Yellow River flows. In addition, Lanzhou is a river valley city located along a river with a width of nearly 300 m, and it is sandwiched between mountain ranges on the north and south banks. The diurnal temperature difference causes air flow between the variations in elevation, resulting in a significant cold lake effect. This leads to higher wind speeds and lower humidity in the city. In recent years, the intensified winter winds and deteriorating living environment in the Lanzhou basin interact with the cold lake effect, resulting in a more adverse microclimate in the city, which is unpleasant for residents [2]. Vegetation is capable of attenuating the cold lake effect and the ridge heating effect, and thus, vegetation is an effective measure for improving microclimate.

Microclimate refers to a climate characterized by differences in heat and water budgets due to differences in the structure and properties of underlying surfaces, resulting in the formation of a climate with different characteristics from the macroclimate on a small scale. Microclimate conditions include factors such as temperature, precipitation, humidity,

wind, and radiation [3]. Numerous studies have reported that vegetation is the primary climate modifier in urban areas [4–7]. Vegetation can reduce air temperature by providing shading and evapotranspiration, which helps to cool the urban environment [8]. Leaves and branches reduce the amount of solar radiation that reaches the area under the tree canopy or plants. Different locations and variations in tree conditions in terms of air temperature and relative humidity values [9], or the optimization of outdoor comfort conditions for different geometric layout configurations, can have different impacts on microclimate, and a well-organized planting layout can improve microclimate [10–12]. Furthermore, a reasonable layout within a green space can significantly decrease wind velocity, improve human comfort, and contribute to the microclimate, ultimately optimizing the living environment [2]. Urban open green spaces play a crucial role in providing thermal comfort and promoting the well-being of urban residents [13]. Therefore, it is necessary to optimize these spaces to improve thermal comfort, especially in cold climate regions, such as high-latitude areas.

Recent studies have demonstrated the potential of parametric optimization in improving thermal comfort in urban green spaces. Factors such as plant selection, layout design, and shading systems can all be optimized to enhance thermal comfort levels. This study contributes to this growing body of knowledge by investigating the effect of different design parameters on thermal comfort in a cold region of China [14]. The recognition of outdoor thermal comfort as a crucial performance indicator for urban-scale environmental assessment has been the focus of several studies that seek to develop effective methods, tools, and indicators to quantify it in various contexts and scales [15]. As part of a global research initiative to standardize the measurement and quantification of outdoor thermal comfort, the Universal Thermal Comfort Index (UTCI) was introduced as a metric [16]. In urban built-up areas, various studies have employed the urban canyon model as the geometrical setting, coupled with one of these thermal comfort indices, to evaluate the impact of various design variables on outdoor thermal comfort.

Software tools play a crucial role in the study of thermal comfort. Recently, the Ladybug Tools suite has emerged as a powerful tool for conducting an extensive parametric analysis of different design choices at a restricted scale [17]. Subsequently, the possibility of modeling outdoor comfort was explored through the integration of a set of tools embedded in the Grasshopper environment, which provides reliable results within reasonable computational time when defining an average urban canopy [10]. This study leverages Ladybug Tools, the plugins of Grasshopper3D, to optimize building height, street width, and orientation to maximize outdoor thermal comfort, which is represented by the diurnal average Universal Thermal Climate Index [18].

Currently, most studies in the field of urban climate focus on investigating the microclimate effects of plants and urban spatial structures under the context of the urban heat island effect during summer. However, a systematic investigation of the microclimate effects of plants with different spatial structures based on the cold lake effect during winter is lacking. In this study, the temperature was aimed to be investigated by the authors alongside humidity and wind speed in various plant configurations during autumn and winter. They analyzed the correlation between plants composition and microclimates under different spatial structures influenced by the cold lake effect. Moreover, the microclimate comfort of three different green open spaces at varying distances from the Yellow River during autumn and winter was assessed by the authors, and the reasons for the observed differences were analyzed. Furthermore, the authors recorded human behavior in different sites and summarized people's preferences, providing insights into the design strategy of microclimate effects of open green spaces (OGSs) in Lanzhou. Finally, the Ladybug Tool was used by the authors to simulate the microclimate comfort in the study area, and fitting analysis was conducted on the measurement results to validate the accuracy of the model in similar temperate river valley cities like Lanzhou and verify the effectiveness of the transformation. In summary, the objectives of this study are to identify the most suitable

green space structure under the cold lake effect from a human perspective and provide a comfortable microclimate environment to improve people's living conditions.

2. Experimental Design

Lanzhou, as a river valley city in the northwest region of China, is characterized by low temperatures and strong winds. It is influenced by various factors such as terrain, geographical location, and monsoon [19]. These factors contribute to hot and windy summers, cold and dry winters, and a relatively low annual precipitation, resulting in an arid and cold climate in the city. According to meteorological data from Lanzhou for the period of 2001–2020 (CDCW, 2020), as shown in Table 1, the average annual temperature is mainly concentrated between 6 and 8 °C. The average annual relative humidity (RH) ranges from 55.0% to 61.0%. A field survey was conducted in a city park in Lanzhou, which is located at a longitude of 103°40' E and latitude of 36°03' N. The measured data for three sampling points are presented in Table 2. Among them, sampling point 1 is closest to the water, exhibiting a temperature difference of 10.7 °C between the maximum and minimum temperatures, with a relative humidity difference of 32.45. Meteorological parameters were measured on site, and the Ladybug Tools tool was utilized to calculate the Universal Thermal Climate Index (UTCI). Questionnaire surveys were conducted among visitors in these spaces to gather personal perception information and spatial perception intentions. The UEG (Urban Energy Game) tool was employed to predict spatial temperature and humidity changes on an hourly basis for one year. The Grasshopper tool was used to construct the spatial models, and the simulation and validation of thermal comfort environments were conducted using meteorological data and UWG (Urban Weather Generator) predictions for the three locations.

Table 1. Average meteorological parameters in Lanzhou city from 2001 to 2020.

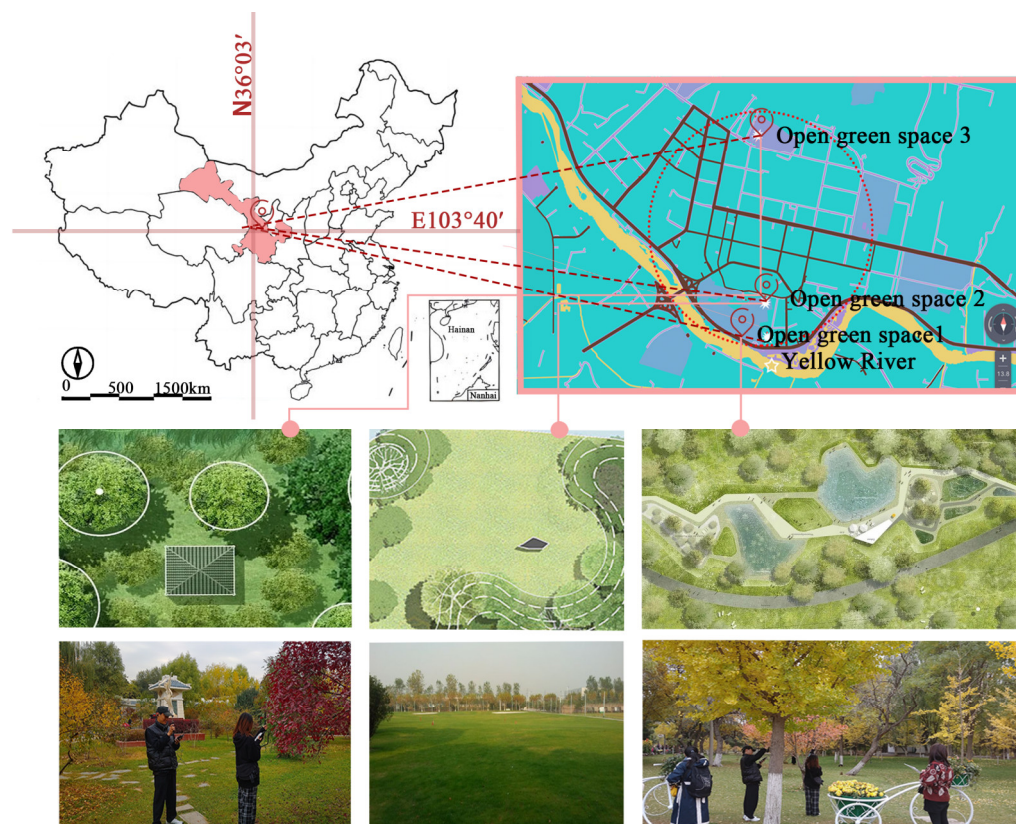
	Average Humidity (%)	Average Wind Speed (m/s)	Average Temperature (°C)	Cumulative Precipitation (mm)	Cumulative Sunshine Duration (h)
2001	57.21	3.79	7.91	292.52	2606.69
2002	57.47	3.65	8.07	299.06	2616.25
2003	60.57	3.84	7.83	382.60	2552.71
2004	56.25	6.01	5.60	292.71	2712.01
2005	56.74	5.24	6.21	306.39	2489.82
2006	57.50	5.23	7.00	272.49	2506.88
2007	60.02	5.17	6.56	423.42	2418.02
2008	59.30	5.09	5.98	336.80	2557.43
2009	56.99	5.16	6.77	270.47	2437.19
2010	57.77	5.36	6.52	282.36	2594.43
2011	58.80	5.08	6.10	274.13	2450.31
2012	59.12	4.94	5.78	357.33	2507.42
2013	53.35	5.05	6.95	320.00	2606.57
2014	58.33	5.20	6.40	393.35	2494.27
2015	56.25	5.33	6.97	264.54	2549.92
2016	56.66	5.33	7.01	362.33	2692.70
2017	57.17	5.00	6.68	361.87	2490.41
2018	59.72	5.06	6.54	504.66	2461.90
2019	60.35	5.10	6.50	402.57	2334.70
2020	57.22	5.18	6.57	347.82	2361.26

Table 2. Measurement of spatial–temporal meteorological variables.

		OGS1	OGS2	OGS3
Va (m/s)	max	0.83	0.79	0.78
	min	0.36	0.33	0.22
	average	0.58	0.55	0.51
Vv (cmm)	max	76.23	71.00	69.12
	min	35.30	34.90	29.00
	average	56.10	54.13	49.34
Tg (°C)	max	14.00	13.70	12.70
	min	3.90	3.98	3.60
	average	8.91	8.20	7.91
Ta (°C)	max	12.50	12.00	11.00
	min	1.80	1.70	1.50
	average	6.58	5.94	5.49
RH (%)	max	56.80	53.00	42.10
	min	24.35	24.00	22.00
	average	41.59	40.29	35.11

2.1. Study Site

Field investigations were conducted during the autumn (7 September and 8 December 2020) and winter (7 November and 7 December 2021) seasons, which corresponded to the coldest and driest periods in Lanzhou. The study areas were located in the Anning District of Lanzhou City, and various green open spaces at different distances from the Yellow River were selected for the investigation (Figure 1).

**Figure 1.** Site locations and measured spaces.

2.2. Meteorological Measurement

Meteorological parameters, namely globe temperature (Tg), air temperature (Ta), relative humidity (RH), and wind speed (Va), were recorded every minute (Table 3). Tg

was recorded using a WGBT-302, while T_a was measured using an anemometer. RH measurements were obtained using a SIGMA AS837 device [11]. In addition, V_v and V_a were measured using a SIGMA AR866A thermal hand-held high-precision digital air volume test and measurement anemometer [14].

Table 3. Technical details of meteorological equipment.

Parameter	Abbreviation	Instrument	Range	Accuracy
Globe temperature	T_g	WGBT-302	0–45 °C	<2%
Wind speed	V_a	Anemometer	0–360°/0~60 m/s	$\pm 3^\circ / \pm 0.3$ m/s
Wind volume	V_v	SIGMA AR866A	0–999,900 m ³ /min	$\pm 1^\circ$
Air temperature	T_a	SIGMA AS837	–10–50°	$\pm 1.5^\circ$
Relative humidity	RH	SIGMA AS837	5%RH–98%RH	$\pm 5\%$ RH (5–40%RH)

The study was conducted during the autumn and winter seasons with experimental observations taking place between 13:30 and 12:00. Measurements of various indicators were taken every 10 min, and the experiment was repeated three times to ensure accuracy. The study encompassed three distinct locations, and specific measurements were obtained from various spaces within each location, including grassland (H), shrub–grass (SH), arbor–grass (AH), and arbor–shrub–grass (ASH) spaces. More detailed information regarding the specific locations and spaces can be found in Appendix A Figures A1–A3, Tables S1–S4.

The mean radiant temperature (T_{mrt}) was calculated on site in terms of the black globe temperature (T_g) and the air temperature (T_a) following the formula:

$$T_{mrt} = \sqrt[4]{(T_g + 273)^4 + \frac{1.1 \times 10^8 \times v^{0.6}}{\epsilon_g \times D^{0.4}} \times (T_g - T_a) - 273} \quad (1)$$

where ($\epsilon_g = 0.95$) and ($D = 0.05$ m) are the globe emissivity and diameter, respectively.

The Universal Thermal Climate Index (UTCI) is a widely accepted parameter for measuring the thermal stress people experience when outdoors. The value of UTCI depends only on wind speed, average radiant temperature, relative humidity and actual air temperature. As calculating the UTCI equivalent temperatures by running the thermoregulation model repeatedly, calculations are performed via an extensive polynomial expression with 210 coefficients [16]. Calculations are performed via an extensive polynomial expression with 210 coefficients. The UTCI can also be calculated by the following simplified equation:

$$UTCI = 3.21 + (0.872 \times T_a) + (0.2459 \times T_{mrt}) - (2.5078 \times V_a) - (0.0176 \times RH) \text{ (}^\circ\text{C)} \quad (2)$$

2.3. Questionnaire Surveys

Questionnaires were conducted simultaneously during the measurement of climatic factors such as wind speed (Appendix A). A total of 600 questionnaires were randomly distributed at 12:00 and 14:00 (± 0.5 h) at the selected location with a total of 509 valid data. The survey questions were based on existing research and are set into three categories in this survey: the first was the personal information of each respondent, including age, gender, means of transportation and type of visitors (the thermal comfort questionnaire is an English translation from the original Chinese).

Part II of the questionnaire explored individual perceptions of different types of activities and thermal sensation, comfort and acceptability. Specifically, activity intensity preference was represented by a list of 5-level scales (low (1); lower (2); normal (3); higher (4); high (5)). Coming here for microclimate comfort was recorded on a 2-point scale (yes

(0); no (1)). Specifically, thermal sensation was expressed by a list of 5-level scales (cold (1); cool (2); neutral (3); warm (4); hot (5)) (Appendix A).

Part III of the questionnaire surveyed strategies of microclimate and space improvement, including wind, humidity, sunshine, plant, architecture, waterscape and people. And it also explored people's perceptions of the frequency of special weather (such as sandstorm, rainstorm, hail, extreme drought and extreme low temperature). Frequency was represented by a list of 5-level scales (many (1); more (2); general (3); less (4); few (5)). (Appendix A).

2.4. Presentation of the Simulation Workflow in Grasshopper

The initial step involved in this study was to procure a suitable weather dataset from available sources in "epw" format, which is widely compatible with a variety of simulation tools. And the authors selected the full year data for the study time based on the ".epw" format data. The Urban Weather Generator (UWG) is a tool utilized in this study, which is designed to estimate urban canopy air temperature and relative humidity on an hourly basis. To achieve this, it takes into consideration various factors such as heat exchange and air stratification in different atmospheres [20,21]. The parameters used in the study include V_a , RH, T_a , T_g , Sunshine (S_s), and UTCI, which were obtained from a 3D model of the study area, which was constructed using Rhinoceros. These values were considered to be representative of the urban scale, and were easily incorporated into the workflow using the graphical interface provided by the Ladybug tool within the Grasshopper environment. This enabled seamless integration with other components of the proposed workflow.

In the final part, the Ladybug tool was employed to simulate the primary influence of wind elements on the environment. Approaches available in Grasshopper include wind analyses using Butterfly [11] or Eddy3D [14] which produce wind factors, the ratio between the simulated wind speeds and the inlet wind speed generated from a number of directions. In this study, Ladybug in Grasshopper was found to be faster, more accurate, and suitable for wind analysis. The workflow diagram for the development and testing of Ladybug is shown in Figure A1, highlighting the connections between different tools. The first step of the proposed simulation workflow was to create an appropriate geometric representation of the urban area under study.

3. Results

3.1. Deceptive Analysis

3.1.1. Measured Meteorological Parameter

Meteorological variables of 10 species of single arbor (A) and single shrub (S) measured during autumn and winter are listed in Appendix B. V_a , V_v of A, S, T_a , T_g and RH all increased significantly. Based on onsite meteorological measurements and field surveys of plant communities, it has been observed that *Cornus chinensis* and *Ligustrum lucidum* are dominant tree species in the local area. Their robust branches and dense foliage contribute to their strong wind resistance, enabling them to effectively withstand strong winds [22]. *Picea asperata* exhibits the strongest thermal insulation due to its needle-like structure. *Ilex rotunda*, with its thicker wax-coated leaves, helps reduce water loss, resulting in its strong moisturizing ability.

Meteorological variables of the four planting patterns measured during autumn and winter are listed in Appendix A. The order of cooling ability of the four planting patterns was arbor and grass (AH) > arbor–shrub–grass (ASH) > shrub–grass (SH) > grass (H). The order of moisturizing ability of the four planting modes was AH > ASH > SH > H. It shows that the shrub has a certain humidification effect, but it is smaller than that of the arbor. The order of wind resistance of the four planting modes is ASH > AH > SH > H. Because of the wind-blocking ability of shrubs, AS and ASH had the strongest wind-blocking ability. H had the weakest wind-blocking effect, and the grass hardly affected the air flow at the pedestrian level. Through the analysis of dynamic Stream Chart and dynamic Ridgeline plots, the V_a and V_v of the three OGSs increased significantly with the seasons, while the

Ta, Tg and RH decreased significantly with the seasons. In the three OGS, RH, Va and Vv decreased significantly with the distance from the Yellow River, while Ta, Tg, MRT and UTCI increased significantly (Figure 2). Significant differences in meteorological variables among the three spaces and the four planting patterns were determined through post hoc Tukey tests (Figure 3). The Va near the Yellow River for two OGSs was significantly different in winter and autumn ($p > 0.05$). The RH of all three OGSs was significantly different in winter.

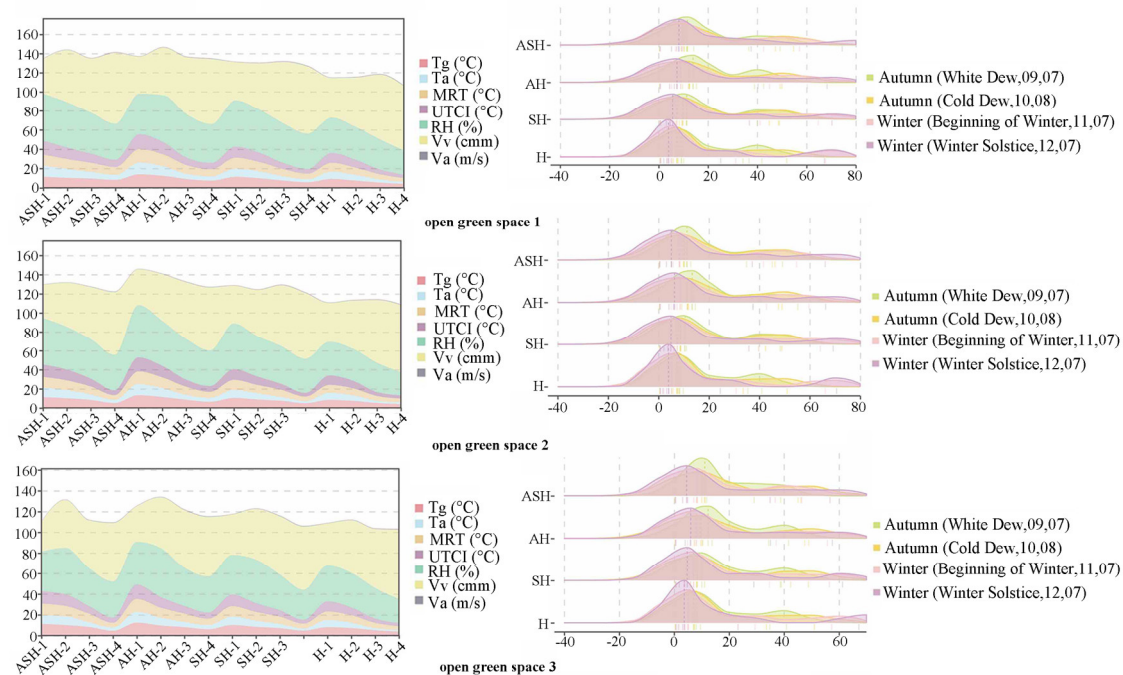


Figure 2. Dynamic Stream Chart and dynamic Ridgeline plots. The X-axis of the three graphs on the left represents “the sampling point numbers of the Qiaoguan grass”, while the Y-axis represents “Globe Temperature (°C), Air Temperature (°C), Mean Radiant Temperature (°C), Universal Thermal Climate Index, Relative Humidity (%), Velocity of Air Motion (cmm), and Air Velocity (m/s)”. The X-axis of the three graphs on the right represents the four seasons, while the Y-axis represents “the sampling point numbers of the Qiaoguan grass”.

3.1.2. Respondent Attributes

A total of 509 effective questionnaires were collected, including 166 in OGS1, 148 in OGS2 and 195 in OGS3. Respondents were composed of 50.69% females and 49.31% males, 22.40% seniors (>55 years old), 67.78% adults (18–55 years old) and 9.82% children (<18 years old). In trials, the majority of respondents reported intensity perceptions for different activity types and perceptions of comfort in different spaces (Figures 4 and 5). At the same time, the perception of Lanzhou’s special weather and suggestions for space renovation were also reported for respondents.

1. Effects of physical factors

Among physical factors, the effects of Ta, RH and Va on the thermal perception of the human body were considered [23]. In this study, all meteorological parameters influenced the thermal sensation of respondents. In OGS1, Va had the highest correlation with thermal sensation among respondents, followed by Ta and RH then G in order. In OGS2, Ta and RH had the highest correlation with thermal sensation among respondents, which was followed by Va and then G in order. In OGS3, Ta and RH had the highest correlation with thermal sensation among respondents, which was followed by Va and then G in order.

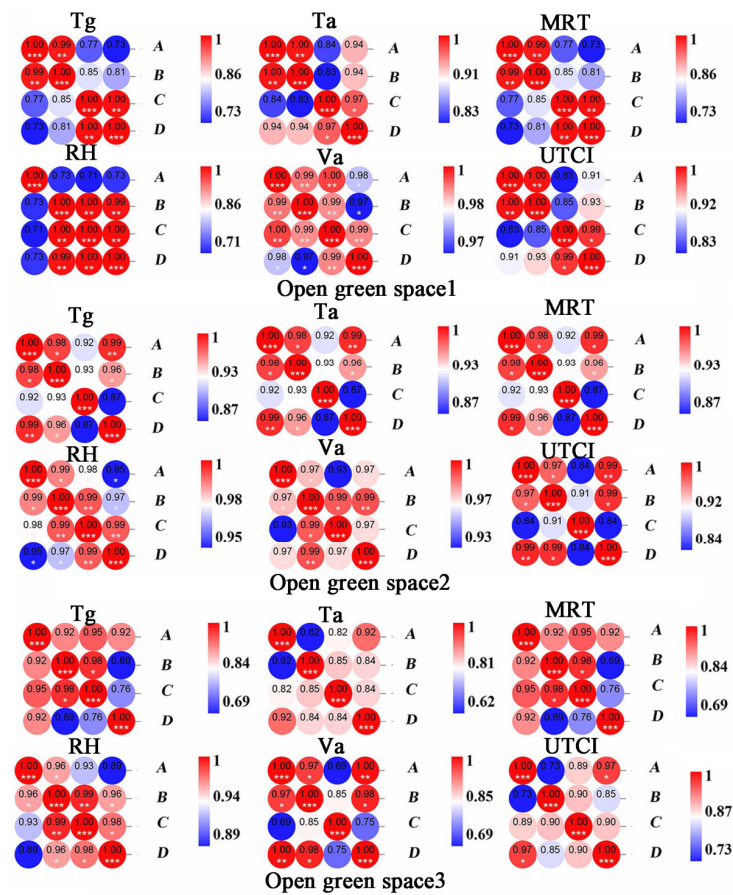


Figure 3. A post hoc Tukey’s test for different pairs of measurement points for the meteorological variables (ASH, AH, SH and S). A–D stand for different times, 09,07, 10,08, 11,07, 12,07; * $p < 0.05$ ** $p < 0.01$. (***) is the significance difference analysis, the more * the more significant the difference).

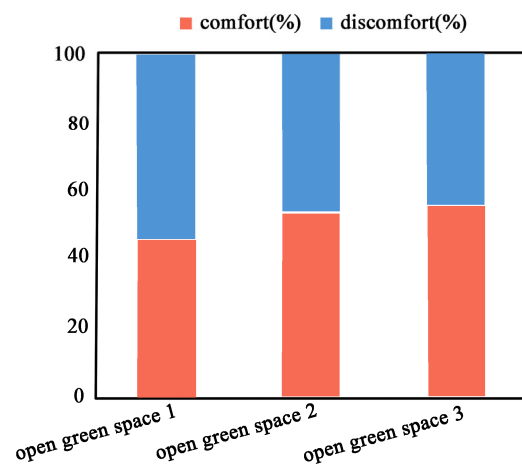


Figure 4. The comfort level of respondents in different spaces.

2. Effects of individual factors

Among individual factors, effects of age, gender, and activity level on the thermal perception of individuals were considered [22]. In this study, there were effects of individual factors on thermal microclimate comfort for respondents. In OGS3, the thermal comfort of microclimate for respondents was influenced by personal activities. The mode of transportation had a negative impact on perceptions of comfort.

3. Landscape elements

In this study, people’s perceptions of the comfort of small environments such as squares, trees, lawns, roads, watersides, buildings, etc. were interviewed by the authors (Figure 6). Discovered by analysis, the comfort of grass space for respondents is affected by the gender in OGS1. The comfort of the waterside is affected by activity. In OGS2, the comfort of grass space for respondents was affected by the Ta and RH. The comfort of architecture was affected by the gender. In OGS3, landscape elements did not have a statistically significant effect on respondents’ comfort level.

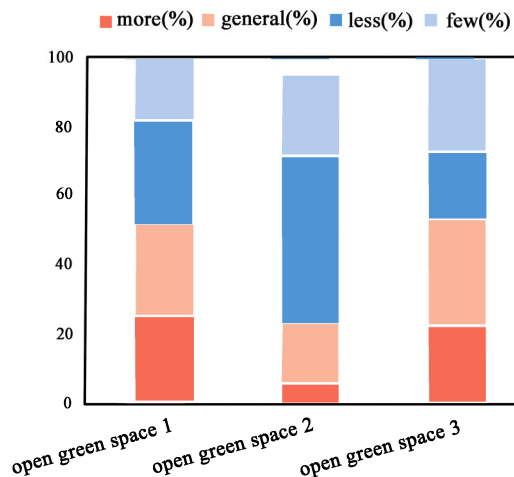


Figure 5. Respondents’ perception of extreme weather in different spaces.

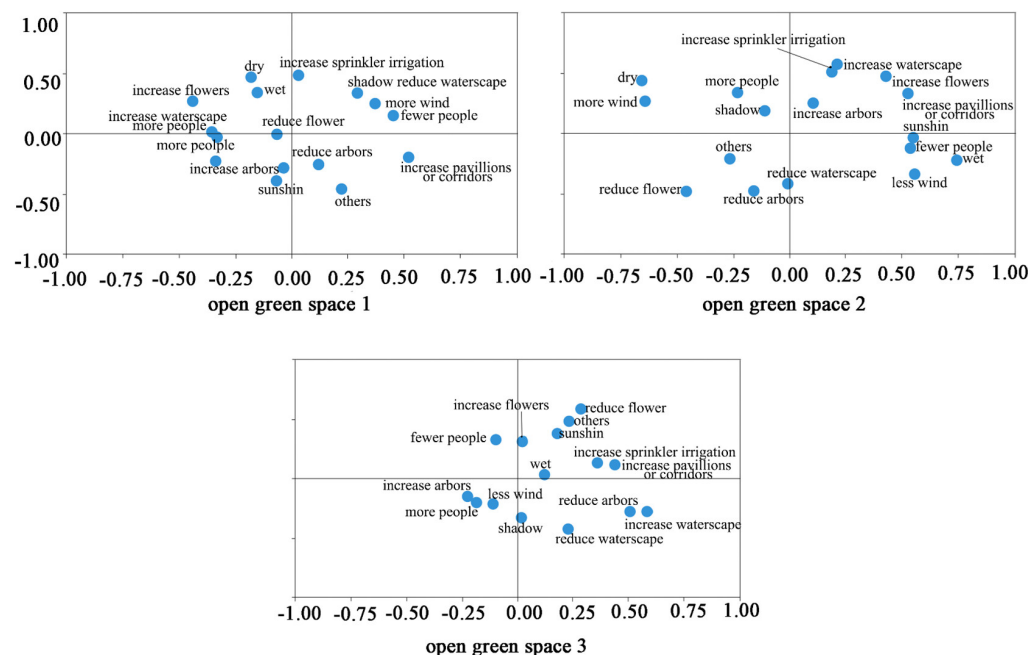


Figure 6. Respondents’ opinions on renovation of different spaces.

3.1.3. Va and RH Simulation in the Model

To validate the reliability of the Ladybug tool in calculating outdoor relative humidity and wind speed, probes were used to apply the same profiles of relative humidity and wind speed within self-built models. The simulated temperature and humidity results for the three spaces were obtained. Wind speed (Figure 7a) and relative humidity (Figure 7c) are simulated through three green space models. It can clearly be seen that although the parameters Va and RH have some discrepancies with the measured values, the fitting degree is high and there is consistency (Figure 7b,e). The results show that there is a strong positive correlation between different spatial measurements and model outputs

Va and RH, $R^2 = 0.986$ (Figure 7c), $R^2 = 0.984$ (Figure 7f). It can clearly be seen that although the parameters Va and RH have some discrepancies with the measured values, the fitting degree is high and there is consistency. The results show that there is a strong positive correlation between different spatial measurements and model outputs Va and RH, $R^2 = 0.986$, $R^2 = 0.984$ (Figure 7a–d).

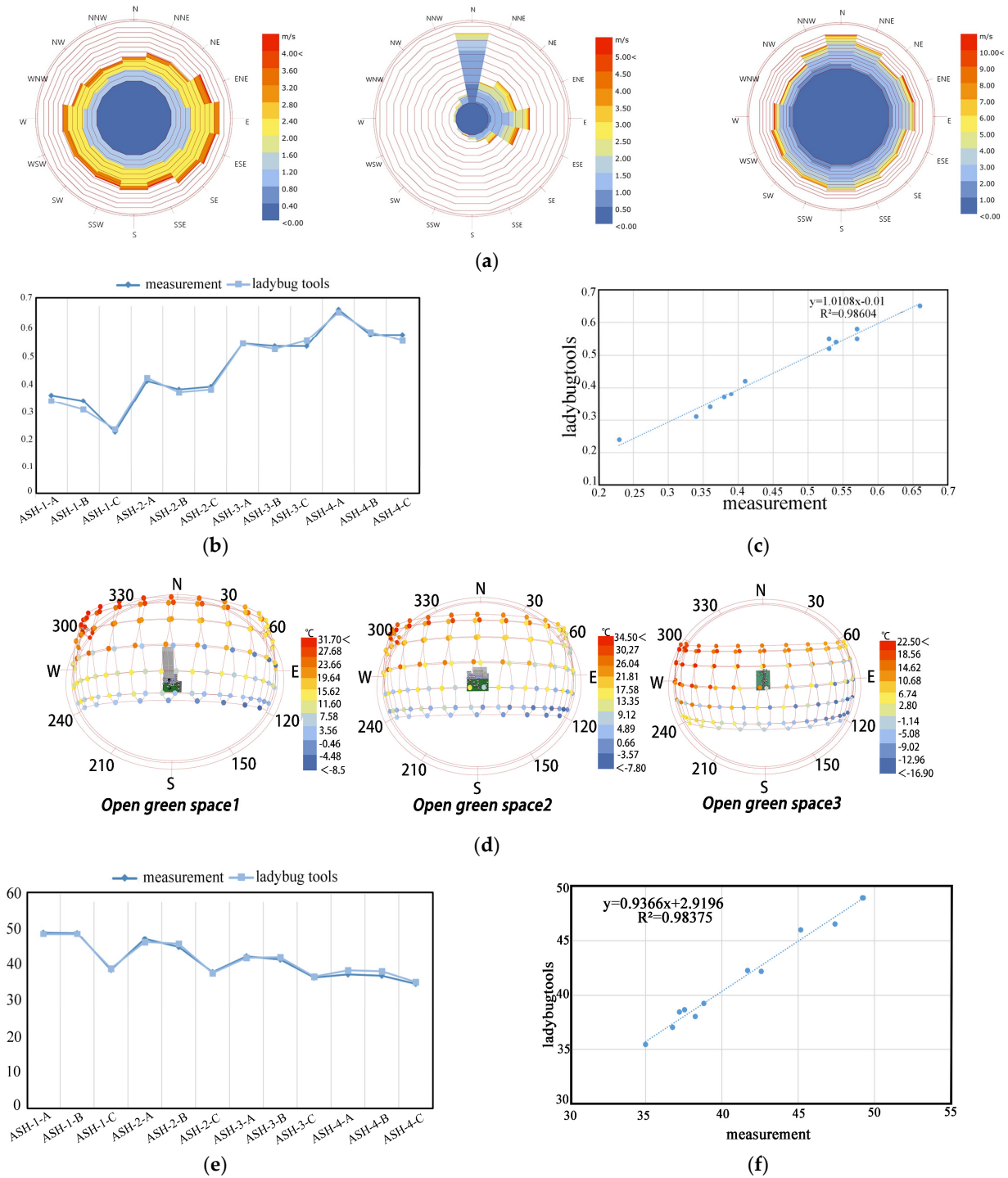


Figure 7. (a) Wind speed simulation results. (b) Relationships between measured and simulated Va. The X-axis represents the sample point number, while the Y-axis represents air velocity. (c) Simulation results of air velocity. (d) Relationships between measured and simulated RH. (e) Relationships between measured and simulated RH. The X-axis represents the sample point number, while the Y-axis represents relative humidity. (f) Relative humidity simulation results.

3.1.4. UTCI Simulation in the Model

It can be clearly seen that the parameter UTCI is in good agreement with the field measurements. The results show that the Ladybug Tools workflow simulates the thermal performance of the geometric configuration with considerable reliability and a short simulation time. Therefore, it can be used for the environmental simulation of the studied locations in this research. The simulation results represent the temperature variations for each hour of every day throughout the year for the three spaces. Although there is some discrepancy between the UTCI parameter and the measured values, there is a high level of fit and significant consistency with an R-squared value of 0.936 (Figure 8).

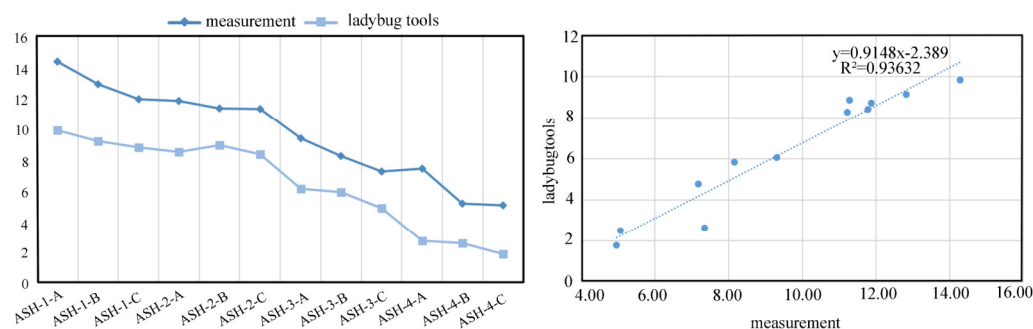


Figure 8. Relationships between measured and simulated UTCI.

3.1.5. Implications for Designers

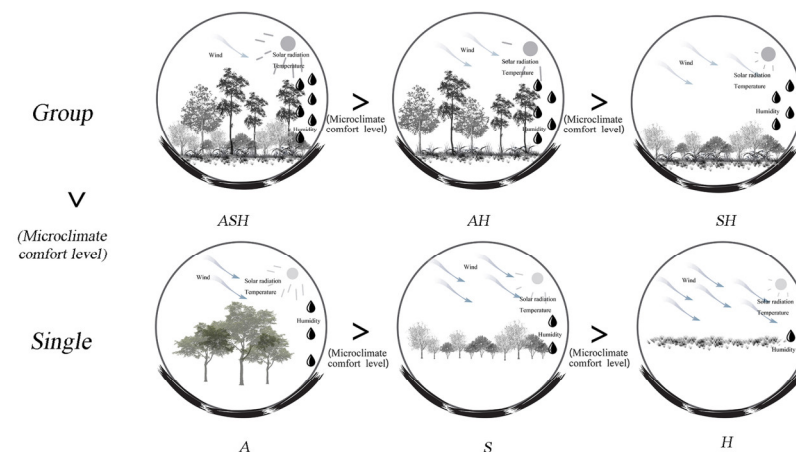
In Lanzhou, due to the cold lake effect of the Yellow River, the outdoor thermal perception of scenic open spaces was mainly influenced by wind. Therefore, it was a great opportunity to improve outdoor comfort by implementing an optimized design of landscape features. Through the joint verification of actual measurement and simulation, it was concluded that in order to cope with the low temperature and minimum precipitation in the autumn and winter seasons, tree species with strong insulation and moisture retention capabilities should be given priority consideration in the design. At the same time, the analysis revealed a negative correlation between activity levels and respondents’ thermal comfort, emphasizing the importance of providing comfortable activity spaces in design. In addition, our simulation results indicated that there was an important connection between an individual’s thermal adaptation ability and the spatial environment. These results were further elaborated in Table 4 and Figure 9. Research on the thermal comfort of grouped and single plants indicated the following microclimate comfort levels: ASH > AH > A and A > S > H (Figure 9a).

Table 4. Bioclimatic design strategies suitable for scenic open spaces in urban areas.

Space	Influencing Factors	Optimal Design Strategies
OGS1 Take ASH space as an example	<p>Closest to the Yellow River, the cold lake effect is the most obvious.</p> <p>Windy, high wind speed, large air volume; fewer trees that reduce wind speed in winter.</p> <p>The spatial distribution of shrubs, arbor and grass is unreasonable.</p> <p>The entrance of the plot faces the Yellow River, and the entire space lacks plant enclosures and wind shields.</p> <p>With less precipitation in winter, plants need increased post-maintenance.</p>	<p>Reduce shrubs and improve natural ventilation.</p> <p>Increase large evergreen trees.</p> <p>Increase the number of fountain pools.</p> <p>Install outdoor spraying equipment.</p> <p>Increase lawn irrigation facilities.</p>

Table 4. Cont.

Space	Influencing Factors	Optimal Design Strategies
OGS2 Take ASH space as an example	<p>Close to the Yellow River, there is a certain cold lake effect.</p> <p>Windy, few trees that reduce wind speed.</p> <p>In winter, the temperature is low and there is a lack of tree species with strong thermal insulation ability.</p> <p>There is little precipitation in winter.</p> <p>There are shelters around the space, which is not conducive to natural ventilation.</p> <p>There is not enough space for activities.</p>	<p>Increase large evergreen trees.</p> <p>According to the research of single tree and single irrigation, choose <i>Syringa oblata</i> to increase the ambient temperature, and choose <i>Prunus cerasifera f. atropurpurea</i> and <i>Syringa oblata</i> to save water.</p> <p>Reduce the space between tree pools and increase the area of seating shade and event space.</p>
OGS3 Take ASH space as an example	<p>Far from the Yellow River, the cold lake effect is not obvious.</p> <p>In winter, there is less precipitation, the lowest humidity and the lowest temperature in the grassy space.</p> <p>There is a certain wind in winter, there are no trees, and it is impossible to block the wind.</p>	<p>Add large evergreen trees, which can be planted alone, or in 3–5 clusters, to ensure lawn space but also provide a certain wind resistance.</p>



a. landscape planting arrangement

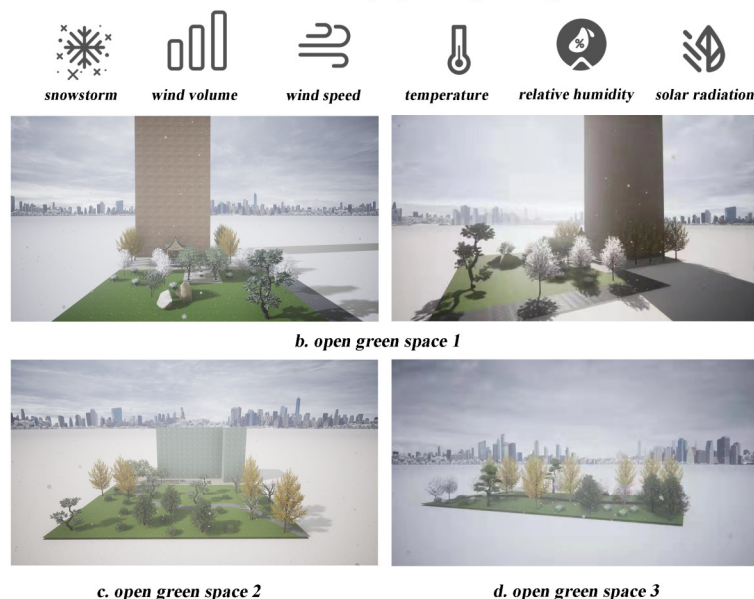


Figure 9. Schematic diagram of bioclimatic transformation.

3.1.6. UTCI after Retrofit

In order to investigate the effects of snowstorm, wind volume, wind speed, temperature, relative humidity and solar radiation on the thermal comfort of small environments, three open green spaces models were established using Rhino (Figure 9). The results show that the Ladybug Tools workflow simulates the thermal performance of the geometric configuration with considerable reliability and a short simulation time; therefore, it can be used in this study. Three open green spaces (ASH) were transformed to simulate comfort after modeling. It was found that the UTCI values were higher than before the transformation (Figure 10). By utilizing the Ladybug tool, simulations were conducted for three open green spaces. Six different perspectives were captured within the software to calculate the Universal Thermal Climate Index (UTCI) for the developed models of these three open green spaces. The x-axis represents the months from January to December, while the y-axis represents the UTCI values. From the graph, it is evident that the red areas are predominantly concentrated in July and August, indicating that the optimal thermal comfort is mainly observed during these two months. Furthermore, the comfort levels among the three open green spaces are comparable, indicating that the renovation efforts can alleviate the heat island effect (Figure 11). In addition, the authors simulated the site sunshine through the model. According to Figure 12, the legend indicates the UTCI values, where colors closer to red represent higher UTCI values, while cooler colors indicate lower UTCI values. It was found that the Ss values of the three green spaces were not much different, which was consistent with our conjecture (Figure 12).

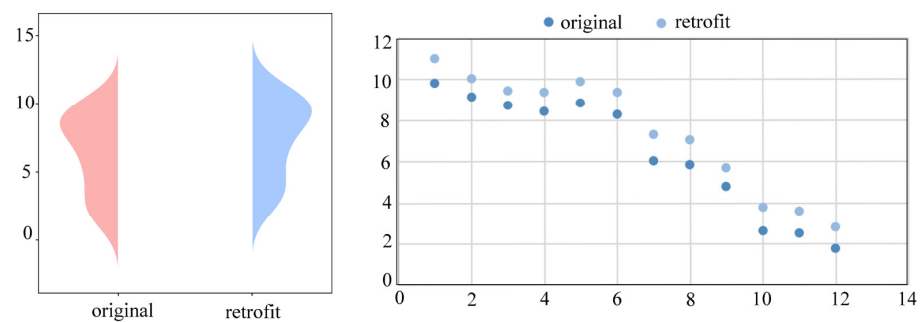


Figure 10. Compare original and retrofit UTCI.

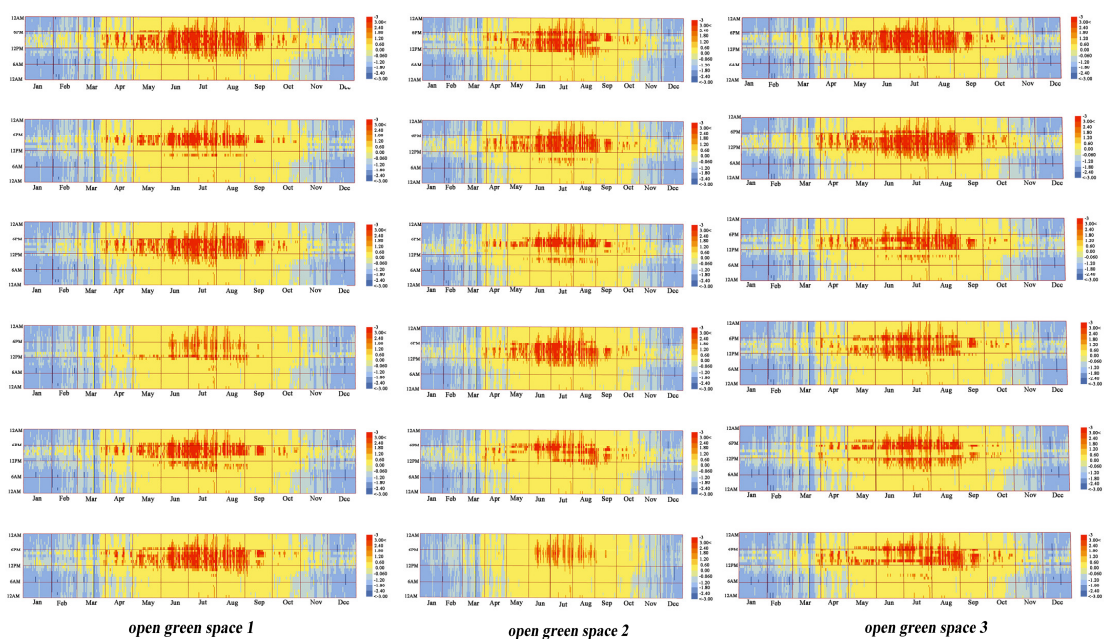


Figure 11. UTCI simulation result.

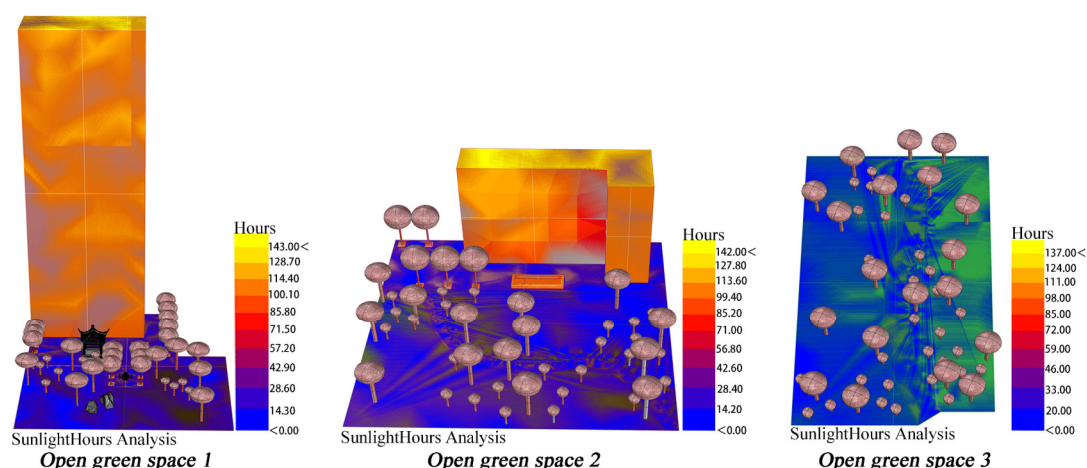


Figure 12. Retrofit sunshine.

4. Discussion

4.1. Factors Affecting Thermal Comfort

Due to the prominent winter microclimate problems in northern China, Lanzhou is cold and long in winter and cools down quickly in autumn. The research is discussing the relationship between different plant configuration patterns and the local microclimate environment in open green spaces at different distances from the Yellow River, which is mainly for the analysis and research of the measured climatic conditions in autumn and winter.

4.1.1. Physical Factors

The present study evaluates the efficacy of different plant configurations in creating environmental comfort. Specifically, it is found by the authors that when a single plant type is employed, trees have the greatest potential to enhance thermal comfort conditions. On the other hand, composite structure types, such as arbor and grass combinations, exhibit the most significant impact on cooling and humidity. Furthermore, the combination of arbor, shrub and grass is found to be most effective in terms of average wind speed and wind-blocking ability in urban green spaces. Notably, our research supports the notion that dense tree coverage is conducive to mitigating heat stress, although vegetation may negatively affect wind ventilation [23,24]. Moreover, our study reveals that changes in relative humidity (RH) are inversely proportional to mean radiant temperature (MRT) and ambient temperature (T_a) during the winter solstice, which is the coldest season in Lanzhou. This finding is consistent with prior research that has shown that the cold lake effect of the Yellow River significantly influences wind conditions in the region during winter [25]. In addition, the authors observed that in OGS1, the thermal sensation of the respondents was most closely related to the air velocity (V_a), indicating the significant impact of the UHI (cold lake effect) [26], which is a climatic phenomenon commonly observed in river valley cities at middle to high latitudes. Conversely, on OGS2–3, thermal sensation was most closely correlated with T_a and RH, followed by V_a , suggesting that these meteorological factors play a crucial role in influencing thermal perception. Therefore, our results highlight the importance of considering strategies to manipulate V_a during the design of outdoor spaces [27].

4.1.2. Individual Factors

The perception of thermal thresholds is influenced by various demographic factors, such as age, gender, and test site [28,29]. However, the present study did not identify any significant effects of individual factors (age and gender) on the thermal microclimate comfort of the respondents. Nevertheless, there were discernible differences in comfort levels across the various test sites. The thermal comfort of respondents in OGS1–2 was

not associated with individual factors. However, in OGS3, the thermal microclimate comfort of respondents was found to be influenced by their activity levels. Specifically, the respondents' mode of transportation to the test site was observed to negatively impact their perception of comfort. This could be attributed to the location of OGS3 on the outskirts of the city, far from the Yellow River, which required respondents to undertake a high level of activity to reach the test site [30].

4.1.3. Environment Factors

The impact of high-rise buildings on microclimate has been well documented in the literature [30]. In the present study, gender was found to influence architectural comfort in OGS1, which is consistent with the fact that this site has the highest number of high-rise buildings among the three test sites. Microclimate perception within the enclosed space of high-rise buildings was found to be inconsistent. A study conducted in Changsha, China, investigated the microclimate of two public squares and explored the effects of buildings, trees, water, and landscape design on improving thermal comfort [31,32]. Within our study, significant differences in respondents' perception of comfort in grass spaces were observed within OGS2. In OGS1, thermal and humidity factors (T_a and RH) were found to influence comfort in grass spaces. However, the dry and cold climate during autumn and winter may not provide adequate improvement in environmental temperature and humidity within the open grassland spaces [33].

4.2. Microclimate Simulation Parameters

The ladybug tool model was chosen for this study to simulate micro environmental climates for several reasons: it is considerably less time consuming to perform calculations, allowing for the simulation of climatic factors for various plant configurations, including RH, T_a , T_g , V_a , Sunshine and UTCI, which are focus on this study, and the ability of parameterization model various spatial shapes, and visualize the results in the Grasshopper environment.

The Ladybug Tools model was selected to simulate micro-environmental climates for several reasons. Firstly, it allows for the simulation of climatic factors for various plant configurations, including relative humidity (RH), air temperature (T_a), globe temperature (T_g), wind velocity (V_a), sunshine, and Universal Thermal Climate Index (UTCI), which are the focus of this study. Secondly, the Ladybug Tools model considerably reduces the time required to perform calculations. Thirdly, it enables the parameterization of various spatial shapes and visualization of the results in the Grasshopper environment.

The Ladybug Tools model is a combination of Grasshopper plugins that estimate outdoor thermal comfort through graphical representation. The model connects Grasshopper to proven software engines that individually calculate thermal comfort determinants. For instance, Honeybee links Grasshopper with EnergyPlus [34] to calculate surface temperatures, while Dragonfly uses the Urban Weather Generator (UWG) [19] to calculate urban air temperature and relative humidity. In this study, Lanzhou city's weather data in "epw" format was used, and the Ladybug component was used to visualize environmental data and output results. The simulations of T_g , T_a , and RH were compared with measured results, which demonstrated strong correlations of $R^2 = 0.996$, $R^2 = 0.997$, and $R^2 = 0.984$, respectively. Although the Butterfly plugin could integrate Open FOAM software (OpenFOAM 9) for computational fluid dynamics (CFD) air-flow analysis, it requires significant computation time. Therefore, the wind speeds in this study were retrieved from weather files, which still demonstrated a strong correlation of $R^2 = 0.986$.

The present study employs a rigorously validated software engine to determine the mean radiant temperature (MRT) and thermal comfort components. In this study, weather data for Lanzhou city in "epw" format was used, and the Ladybug component was employed to visualize the environmental data and output results. The simulation results of T_g , T_a , and RH were compared with the measured values, showing strong correlations with R-squared values of 0.996, 0.997, and 0.984, respectively. The Urban Weather Generator

(UWG) has been validated through field measurements in diverse climates [19,20] and is utilized to investigate how different UTCI components are combined and how the MRT equations are applied, both of which require validation. In a Mediterranean climate context, Evola et al. validated the Ladybug Tools workflow through experimental measurements of MRT in Catania, Italy [35]. Their study reported a coefficient of determination $R^2 = 0.92$ in good agreement with measurements. Additionally, the present study rigorously validates the workflow implemented in Ladybug Tools modeling. As shown in Figure 2, the average UTCI results for all three open green spaces exhibit consistent performance with an R^2 of 0.936. This indicates that the proposed method exhibits good reliability in scenarios with the cold lake effect in middle to high-latitude regions. In similar environmental settings, this simulation can be applied in the early design process to model and assess alternative schemes, aiming to find space design solutions that offer improved thermal comfort while fulfilling other functional requirements. Subsequently, the design can be further refined and implemented during construction.

4.3. Retrofit Strategy

In this paper, through the actual measurement and simulation verification of different vegetation configurations in different open green spaces at different distances from the Yellow River, the design strategy with the best environmental comfort is found. The methodology described in this paper can be replicated and used to test other performance criteria, such as energy loads, through its core simulation engine, EnergyPlus [36]. Grasshopper is very friendly to planners, designers and others without proficiency in programming. There is no doubt that the use of open source plugins and environment plugins in Grasshopper has increased its popularity in climate research and has quickly become an indispensable tool in practice [37]. The method described in this article can be replicated and used to test other performance standards, such as energy load, by utilizing its core simulation engine, EnergyPlus [38].

A comprehensive approach was taken to evaluate the impact of different vegetation configurations on environmental comfort in various open green spaces situated at varying distances from the Yellow River. The methodology outlined in this research can be replicated and extended to examine other performance criteria, such as energy loads, through its core simulation engine, EnergyPlus. Grasshopper, with its open source and environmental plugins, has emerged as a popular and user-friendly tool for planners, designers and researchers without expertise in programming [18]. Our study establishes a close correlation between the T_g , T_a , V_v and RH measurements and simulation results. A visual tool, the “UTCI Rose”, was developed by the authors to analyze people’s perceptions of the comfort of small environments and guide urban designers in creating comfortable outdoor environments. The UTCI values reported in our study provide a direct measure of pedestrian thermal comfort in degrees Celsius, thereby facilitating the incorporation of climate indicators into design guidelines at different scales from districts to small urban areas. The methodology outlined in this study has the potential to contribute to the creation of resilient and sustainable urban environments that ensure pedestrian comfort.

4.4. Limitations

The wind and humidity analysis was performed based on the wind speed and relative humidity in the file, as these variables exhibited high reliability in the workflow. While other methods such as wind analysis using Butterfly or Eddy3D [15] are available in Grasshopper and generate wind factors that simulate wind speed in many directions, they are not as accurate as accounting for turbulent heat exchange in the model, which is a feature in the Open FOAM software currently under development and not yet integrated into either of the two plugins. Additionally, the Ladybug Tools model was found to underestimate the UTCI by approximately 3.5 °C compared to the field measurements, which was mainly due to spatial resolution issues in the plant simulation model that may lead to inaccurate sun occlusion angles. Despite these differences, they remain consistent

under hypothetical cases and are thus acceptable. However, the model requires further refinement for detailed analysis.

5. Conclusions

In this study, a comparison of respondents' perceptions of the thermal environment was conducted in three different types of sites in Lanzhou, China, utilizing different plant configuration spaces. Through the use of meteorological measurements and questionnaires, the physical, personal, and environmental factors that influence the thermal perception of residents and tourists were systematically discussed and compared. The study drew some major conclusions:

- (1) The cooling ability of the four planting patterns was ranked in order of arbor and grass (AH) > arbor–shrub–grass (ASH) > shrub–grass (SH) > grass (H), while the moisturizing ability was ranked in order of AH > ASH > SH > H, and the wind resistance was ranked in order of ASH > AH > SH > H. The values of air velocity (V_a) and vertical air velocity (V_v) increased significantly with seasons in the three spaces, whereas air temperature (T_a), ground surface temperature (T_g), and relative humidity (RH) changed significantly with seasons in the three spaces. Secondly, the change of RH was found to be inversely proportional to the solar radiation (SR) and mean radiant temperature (MRT), and the RH during winter solstice was the smallest in autumn and winter.
- (2) The cold lake effect of the Yellow River dominates the wind environment in Lanzhou, and the wind speed in winter is high. In OGS1, V_a had the highest correlation with respondents' thermal sensation. The residential area is closest to the Yellow River, indicating that the cold lake effect of the Yellow River does cause strong winds in the environment, which has a certain impact on comfort. In OGS2–3, T_a and RH had the highest correlations with thermal sensation among respondents, which were followed by V_a and G.
- (3) The present study highlights the influence of individual factors on respondents' thermal microclimate comfort with notable variations across different sites. Specifically, in OGS2, respondents exhibit significantly diverse perceptions of the comfort of grassy spaces on the campus. In OGS1, gender affects the comfort of buildings, whereas the comfort of grass space is influenced by T_a and RH. Conversely, individual activities have a significant impact on respondents' thermal comfort in OGS3.
- (4) Despite certain discrepancies between the measured values and UTCI parameters, the high degree of consistency and good fitting degree, $R^2 = 0.936$, indicate that the parameters T_g , T_a , V_a , and RH exhibit good agreement with the field measurements, with R^2 values of 0.996, 0.997, 0.986, and 0.984, respectively.

The findings of this study provide insight into the mechanism underlying respondents' thermal perception of the cold lake effect associated with the Yellow River. Furthermore, the site and actual measurement were simulated by the authors using Ladybug Tools, and the renovation plan was verified to achieve people's thermal comfort. The implications of our results and methodology are expected to provide theoretical guidance for urban planners to consider climate-responsive design principles such as vegetation, irrigation, and shading to enhance outdoor comfort for visitors. The high level of fit between the simulated and measured data also indicates the reliability of this method in similar environments. It can be used as a reference in the early stages of design to assess and optimize the thermal comfort of spaces.

Supplementary Materials: The following supporting information can be downloaded at: <https://www.mdpi.com/article/10.3390/buildings13092329/s1>. Table S1. Volunteers' attributes. Table S2. Open green space 1. Table S3. Open green space 2. Table S4. Open green space 3.

Author Contributions: Conceptualization, J.L. and S.J.; methodology, J.L.; software, S.J.; validation, S.Z. and S.Y.; formal analysis, S.Z.; investigation, W.J.; resources, W.J.; data curation, J.L.; writing—original draft preparation, J.L.; writing—review and editing, J.L. and S.J.; visualization, S.J.; supervision, W.L.; project administration, W.J.; funding acquisition, W.J. and W.L. All authors have read and agreed to the published version of the manuscript.

Funding: This research was funded by the Ministry of Science and Technology of China (2019FY101604).

Data Availability Statement: The data presented in this study are available on request from the corresponding author.

Conflicts of Interest: The authors declare no conflict of interest.

Appendix A

Thermal comfort questionnaire (English translation from the original Chinese).

1. Location: _____ Time: _____ Length of time living locally: _____ Hometown: _____ Current wind speed: _____ Current temperature/humidity: _____ Current sunshine: _____ (1, 2, 3 and 4, four levels are enhanced in turn)
2. Gender: _____ Age: _____ Occupation: _____
3. Means of Transportation: () A. Self-driving B. Bus C. Subway D. Taxi E. Shared bike F. Walking
4. Activity type and perceived intensity

	Low	Lower	Normal	Higher	High
Sitting	<input type="radio"/>	<input type="radio"/>	<input type="radio"/>	<input type="radio"/>	<input type="radio"/>
Standing	<input type="radio"/>	<input type="radio"/>	<input type="radio"/>	<input type="radio"/>	<input type="radio"/>
Slow walking	<input type="radio"/>	<input type="radio"/>	<input type="radio"/>	<input type="radio"/>	<input type="radio"/>
Fast walking	<input type="radio"/>	<input type="radio"/>	<input type="radio"/>	<input type="radio"/>	<input type="radio"/>
Ball sports	<input type="radio"/>	<input type="radio"/>	<input type="radio"/>	<input type="radio"/>	<input type="radio"/>

5. Did you come to the venue because of the comfortable climate? Yes No
6. Evaluation of microclimate comfort in different space types

	Cold	Cool	Neutral	Warm	Hot
Square	<input type="radio"/>	<input type="radio"/>	<input type="radio"/>	<input type="radio"/>	<input type="radio"/>
Woodland	<input type="radio"/>	<input type="radio"/>	<input type="radio"/>	<input type="radio"/>	<input type="radio"/>
Lawn	<input type="radio"/>	<input type="radio"/>	<input type="radio"/>	<input type="radio"/>	<input type="radio"/>
Road	<input type="radio"/>	<input type="radio"/>	<input type="radio"/>	<input type="radio"/>	<input type="radio"/>
Waterside	<input type="radio"/>	<input type="radio"/>	<input type="radio"/>	<input type="radio"/>	<input type="radio"/>
Architecture	<input type="radio"/>	<input type="radio"/>	<input type="radio"/>	<input type="radio"/>	<input type="radio"/>

7. Do you feel that the special weather (such as sandstorm, rainstorm, hail, extreme drought and extreme low temperature) in your place is frequent in the current season? many more general less few
8. Your preference for microclimate improvement (four groups, one from each group, four in total, and only four)
 - more wind less wind wet dry sunshine shadow more people
 - fewer people
9. Your preference for space improvement
 - increase trees reduce trees increase flowers reduce flowers increase pavilions or corridors increase waterscape reduce waterscape increase sprinkler



open green space 1

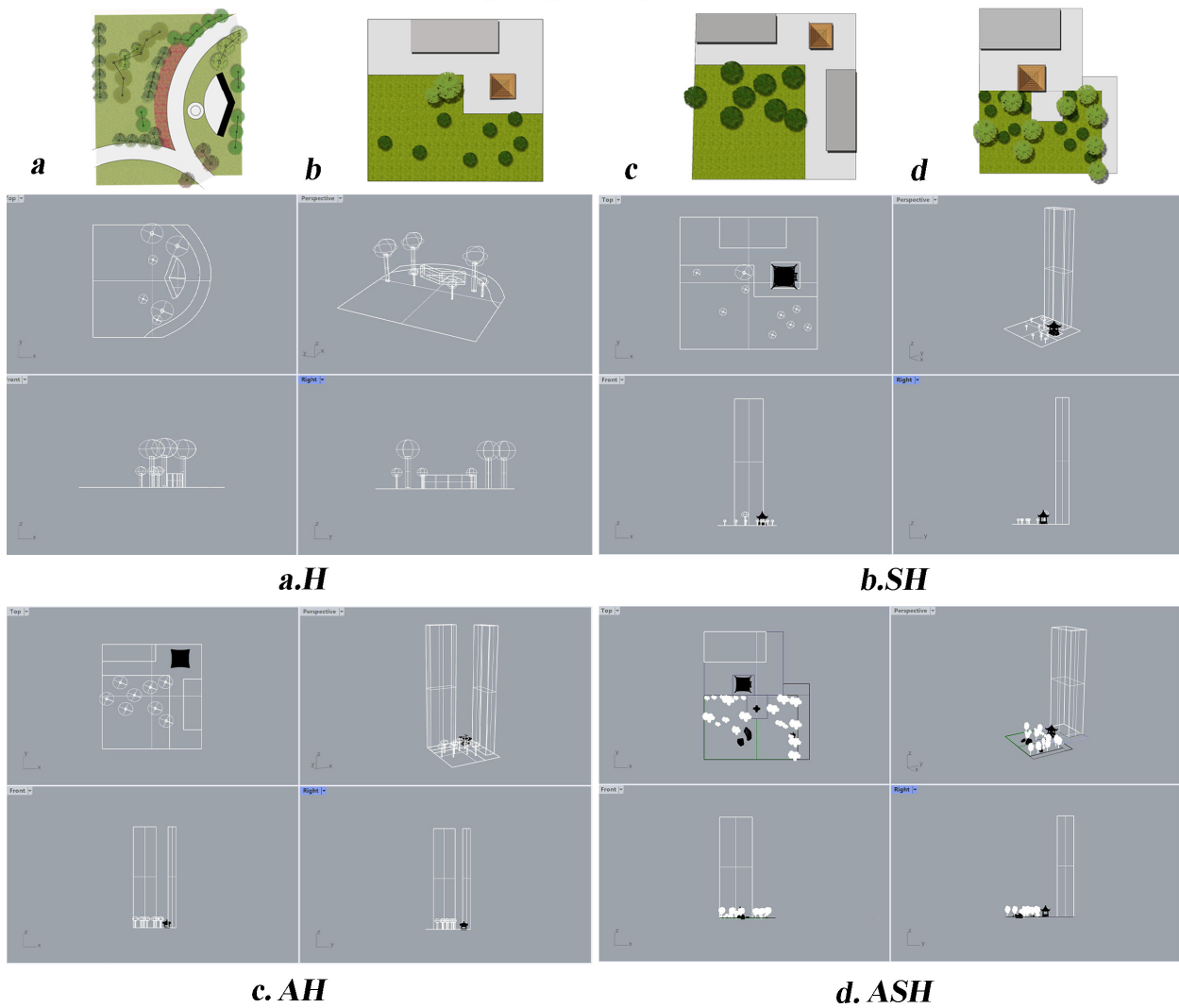


Figure A1. Open green space 1.



open green space 2

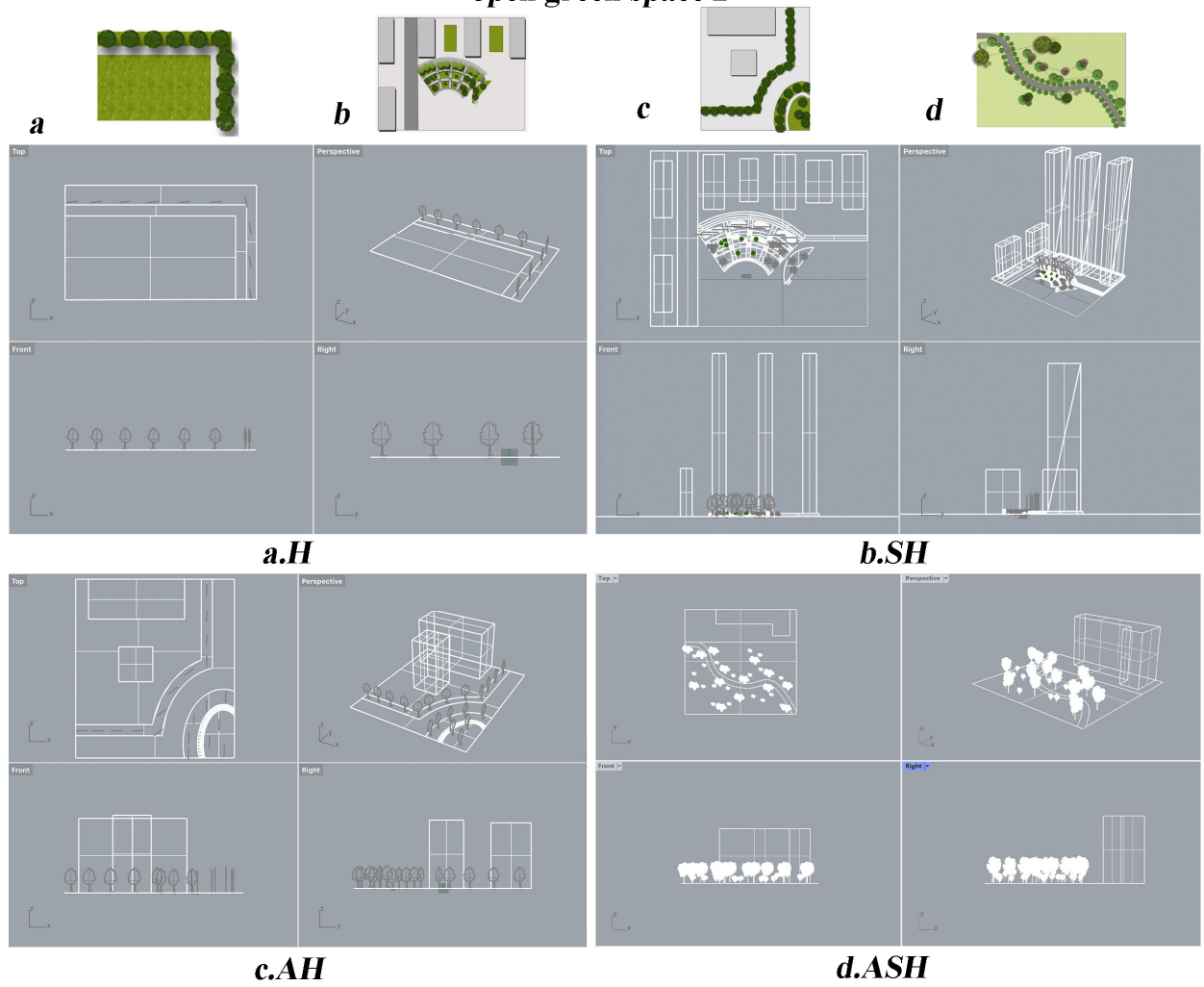
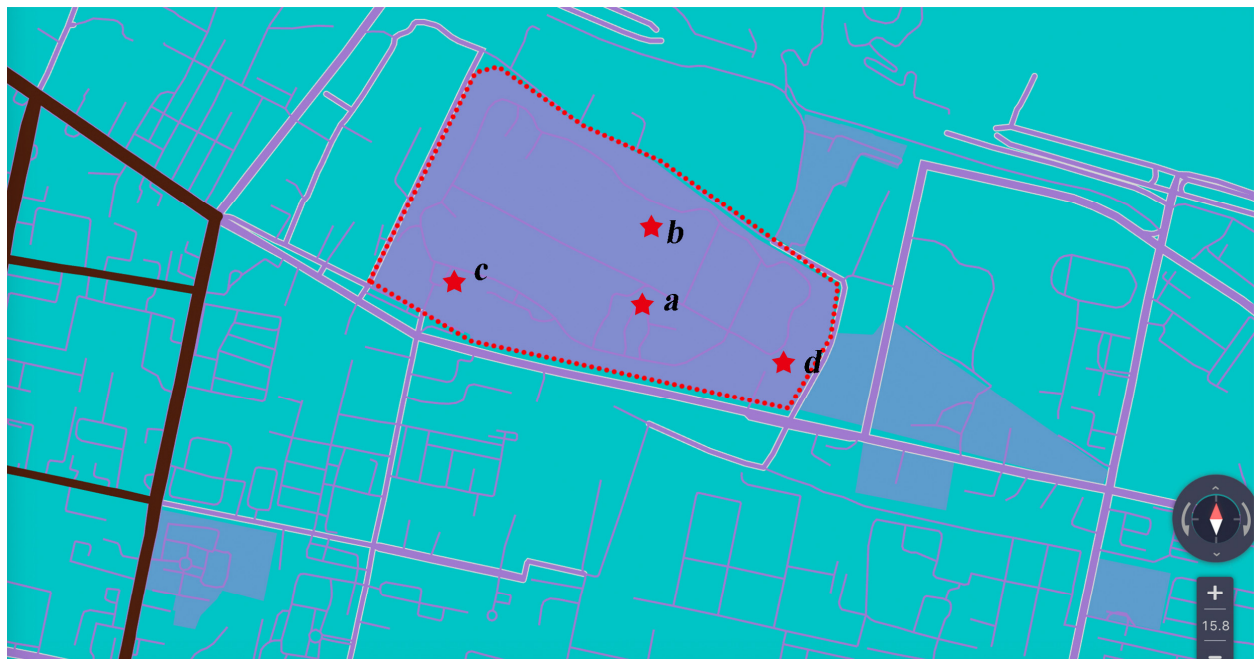


Figure A2. Open green space 2.



open green space 3

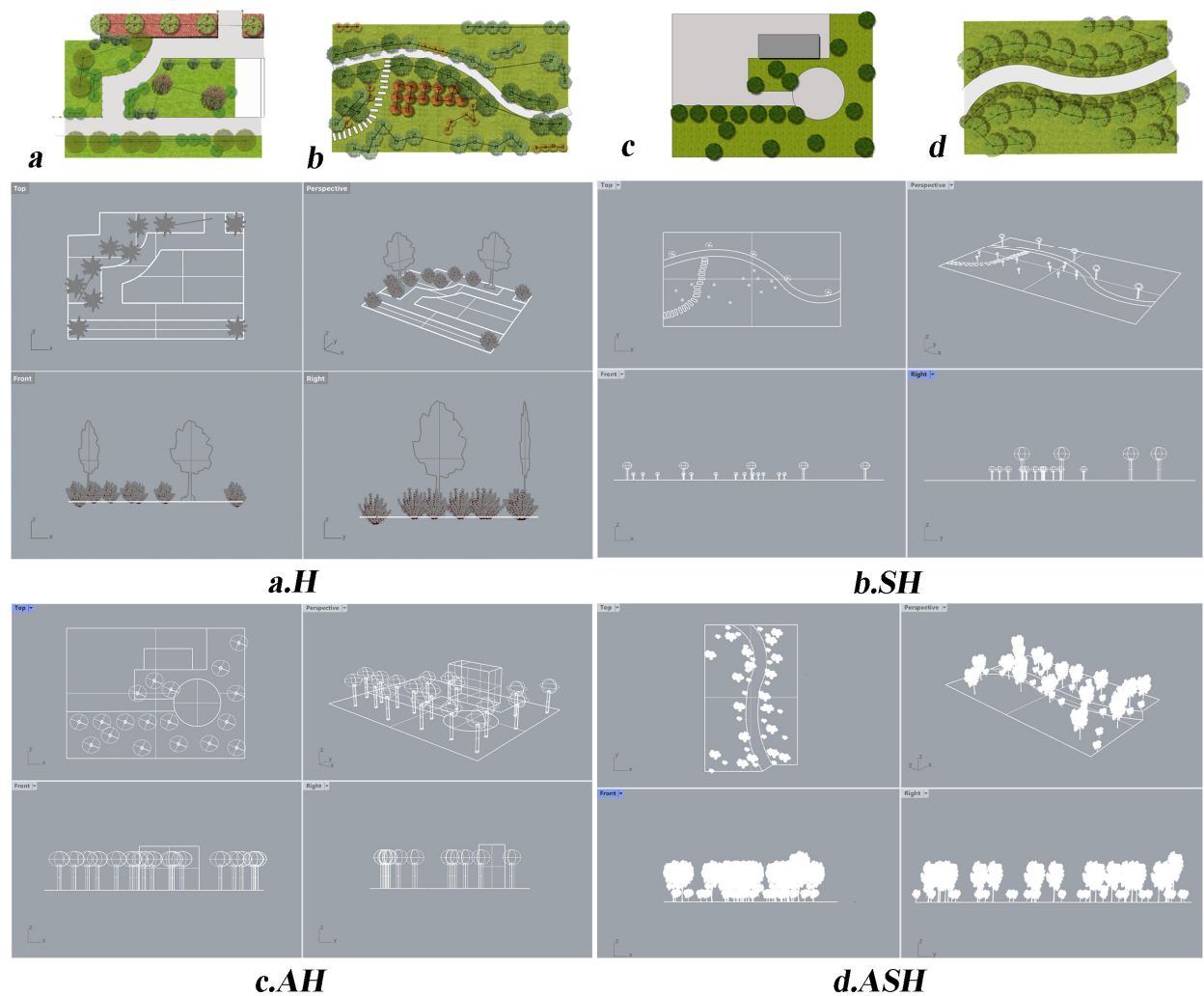


Figure A3. Open green space 3.

Appendix B

Table A1. Meteorological variables in each measured space (Open green space 1).

		Autumn (White Dew, 09,07)	Autumn (Cold Dew, 10,08)	Winter (Beginning of Winter, 11,07)	Winter (Winter Solstice, 12,07)
V_a (m/s)	<i>Juniperus formosana</i>	0.20 ± 0.006 Cd	0.29 ± 0.006 Bbc	0.34 ± 0.186 Bcd	0.46 ± 0.009 Ae
	<i>Buxus megistophylla</i>	0.21 ± 0.006 Bd	0.24 ± 0.23 ABc	0.27 ± 0.067 ABd	0.32 ± 0.009 Af
	<i>Cedrus deodara</i>	0.54 ± 0.012 Ca	0.60 ± 0.012 BCa	0.64 ± 0.012 Ba	0.77 ± 0.153 Aa
	<i>Firmiana simplex</i>	0.39 ± 0.013 Bb	0.58 ± 0.006 Aa	0.60 ± 0.029 Aa	0.68 ± 0.003 Ab
	<i>Picea asperata</i>	0.18 ± 0.006 Cc	0.55 ± 0.006 Ba	0.67 ± 0.021 Aa	0.73 ± 0.007 Aab
	<i>Styphnolobium japonicum 'Pendula'</i>	0.14 ± 0.009 Dde	0.29 ± 0.012 Cbc	0.44 ± 0.021 Bb	0.54 ± 0.003 Ad
	<i>Juniperus chinensis</i>	0.18 ± 0.003 Ce	0.27 ± 0.006 Bc	0.31 ± 0.012 Bcd	0.43 ± 0.012 Ae
	<i>Betula platyphylla</i>	0.16 ± 0.012 Dde	0.29 ± 0.006 Cbc	0.40 ± 0.009 Bbc	0.4 ± 0.007 Ae
	<i>Pinus bungeana</i>	0.18 ± 0.003 Dde	0.35 ± 0.006 Cb	0.47 ± 0.006 Bb	0.60 ± 0.003 Bc
	<i>Prunus cerasifera f. atropurpurea</i>	0.24 ± 0.022 Ce	0.23 ± 0.026 Ccde	0.32 ± 0.015 Bcd	0.46 ± 0.003 Ae
T_g (°C)	<i>Juniperus formosana</i>	6.68 ± 0.058 Bg	9.47 ± 0.035 Ae	5.68 ± 0.058 Cc	3.03 ± 0.037 Df
	<i>Buxus megistophylla</i>	7.68 ± 0.115 Af	6.97 ± 0.059 Bf	6.68 ± 0.115 Bbc	3.75 ± 0.100 Ce
	<i>Cedrus deodara</i>	9.88 ± 0.115 ABe	10.37 ± 0.344 Ade	8.54 ± 0.240 Bab	4.72 ± 0.039 Cbc
	<i>Firmiana simplex</i>	11.62 ± 0.115 Ad	11.57 ± 0.079 Bcd	9.29 ± 0.240 Ca	4.92 ± 0.039 Dab
	<i>Picea asperata</i>	14.82 ± 0.231 ABab	15.56 ± 0.510 Aa	10.59 ± 0.489 Ba	5.16 ± 0.023 Ca
	<i>Styphnolobium japonicum 'Pendula'</i>	15.68 ± 0.058 Aa	15.50 ± 0.137 Aa	9.67 ± 0.947 Ba	4.55 ± 0.029 Cc
	<i>Juniperus chinensis</i>	13.51 ± 0.058 Ac	13.02 ± 0.203 Ab	10.18 ± 0.285 Ba	4.14 ± 0.031 Cdc
	<i>Betula platyphylla</i>	14.09 ± 0.379 Ab	12.15 ± 0.082 Abc	9.14 ± 0.603 Bab	3.55 ± 0.068 Ce
	<i>Pinus bungeana</i>	11.25 ± 0.058 Ad	11.10 ± 0.029 Acd	8.57 ± 0.368 Bab	4.07 ± 0.033 Cd
	<i>Prunus cerasifera f. atropurpurea</i>	11.60 ± 0.173 Ad	11.86 ± 0.449 Ac	10.08 ± 0.139 Ba	3.82 ± 0.093 Cde
T_a (°C)	<i>Juniperus formosana</i>	5.29 ± 0.035 Ah	4.51 ± 0.067 Bf	3.15 ± 0.29 Cde	1.00 ± 0.115 Dc
	<i>Buxus megistophylla</i>	6.41 ± 0.234 Ag	5.93 ± 0.077 Af	3.44 ± 0.04 Bde	1.6 ± 0.305 Cbc
	<i>Cedrus deodara</i>	9.69 ± 0.058 Af	9.44 ± 0.172 Ad	4.79 ± 0.105 Bbc	2.23 ± 0.120 Cab
	<i>Firmiana simplex</i>	13.78 ± 0.058 Ac	13.22 ± 0.563 Ab	5.89 ± 0.064 Ba	2.45 ± 0.029 Ca
	<i>Picea asperata</i>	14.73 ± 0.115 Ab	15.09 ± 0.266 Aa	5.48 ± 0.290 Bab	2.53 ± 0.176 Ca
	<i>Styphnolobium japonicum 'Pendula'</i>	17.78 ± 0.115 Aa	16.35 ± 0.448 Aa	5.11 ± 0.437 Babc	2.15 ± 0.755 Cab
	<i>Juniperus chinensis</i>	14.08 ± 0.310 Abc	13.17 ± 0.138 Ab	4.81 ± 0.064 Bbc	1.93 ± 0.064 aCb
	<i>Betula platyphylla</i>	12.65 ± 0.006 Ad	11.53 ± 0.120 Bc	4.33 ± 0.088 Ccd	1.83 ± 0.035 Dab
	<i>Pinus bungeana</i>	10.72 ± 0.115 Ae	10.22 ± 0.173 Acd	4.19 ± 0.034 Bcd	1.45 ± 0.074 Cbc
	<i>Prunus cerasifera f. atropurpurea</i>	11.23 ± 0.115 Ae	10.74 ± 0.278 Acd	4.17 ± 0.037 Bcd	1.86 ± 0.094 Cbc
RH (%)	<i>Juniperus formosana</i>	60.84 ± 0.462 Aa	59.28 ± 0.577 Aa	54.85 ± 0.356 Ba	47.33 ± 0.362 Cab
	<i>Buxus megistophylla</i>	54.28 ± 1.707 ABc	57.35 ± 1.468 Aa	48.35 ± 0.233 BCc	43.57 ± 0.513 Cc
	<i>Cedrus deodara</i>	49.49 ± 0.450 Ad	45.49 ± 0.577 ABb	42.49 ± 1.154 Bde	35.57 ± 0.384 Ce
	<i>Firmiana simplex</i>	37.06 ± 0.766 Af	36.3 ± 0.058 Ac	34.07 ± 0.521 ABf	31.83 ± 0.273 Bf
	<i>Picea asperata</i>	35.81 ± 0.181 Af	37.47 ± 0.231 Ac	32.90 ± 0.385 Bf	31.08 ± 0.586 Bf
	<i>Styphnolobium japonicum 'Pendula'</i>	38.53 ± 0.312 Af	33.21 ± 0.008 Bc	29.88 ± 0.252 Cg	27.96 ± 0.281 Dg
	<i>Juniperus chinensis</i>	45.38 ± 0.347 Ae	45.03 ± 0.017 Ab	40.36 ± 0.384 Be	35.99 ± 0.564 Ce
	<i>Betula platyphylla</i>	53.28 ± 0.398 Acd	50.53 ± 0.058 Ab	44.36 ± 0.285 Bd	39.15 ± 0.596 Cd
	<i>Pinus bungeana</i>	69.94 ± 0.436 Aa	62.57 ± 0.231 Ba	51.19 ± 0.748 Cbc	45.70 ± 0.439 Dbc
	<i>Prunus cerasifera f. atropurpurea</i>	59.57 ± 0.637 Ab	62.31 ± 3.535 Ab	53.76 ± 0.286 Aab	49.76 ± 0.694 Aa
V_v (cmm)	<i>Juniperus formosana</i>	13.47 ± 0.049 Ce	21.74 ± 0.577 Bc	26.13 ± 0.196 Ac	28.04 ± 0.294 Ade
	<i>Buxus megistophylla</i>	16.45 ± 0.654 Bd	17.83 ± 0.058 Be	19.16 ± 0.338 ABd	20.66 ± 0.172 Af
	<i>Cedrus deodara</i>	39.93 ± 0.126 Ca	42.11 ± 0.577 BCa	44.11 ± 0.577 Ba	47.72 ± 0.434 Aa
	<i>Firmiana simplex</i>	26.66 ± 0.234 Cb	40.93 ± 0.231 Ba	42.11 ± 0.485 ABa	44.42 ± 0.354 Ab
	<i>Picea asperata</i>	21.25 ± 0.598 Cc	40.46 ± 0.231 Ba	43.41 ± 0.516 ABa	45.4 ± 0.468 Aab
	<i>Styphnolobium japonicum 'Pendula'</i>	14.32 ± 0.244 Ce	21.16 ± 0.577 Bcd	25.07 ± 0.093 Ac	27.59 ± 0.581 Ade
	<i>Juniperus chinensis</i>	10.28 ± 0.124 Cfe	18.89 ± 0.346 Bde	24.22 ± 0.647 Ac	26.02 ± 0.690 Ae
	<i>Betula platyphylla</i>	10.43 ± 0.86 Cf	20.67 ± 0.577 Bcd	26.67 ± 0.577 Ac	30.07 ± 0.636 Ac
	<i>Pinus bungeana</i>	11.00 ± 0.299 Df	24.97 ± 0.520 Cb	29.30 ± 0.383 Bb	33.25 ± 0.653 Ad
	<i>Prunus cerasifera f. atropurpurea</i>	13.86 ± 0.200 De	16.26 ± 0.115 Bf	10.14 ± 0.130 Bd	25.29 ± 0.420 Ae

Notes: Values are performed as mean values ± standard errors. The different normal letters in the same column indicate significant differences among treatments at the 0.001 level, while the different capital letters in the same row indicate significant differences among stages at the 0.001 level. The same is shown below.

Table A2. Meteorological variables in each measured space (Open green space 2).

	Autumn (White Dew, 09,07)	Autumn (Cold Dew, 10,08)	Winter (Beginning of Winter, 11,07)	Winter (Winter Solstice, 12,07)	
V_a (m/s)	<i>Berberis thunbergii</i> 'Atropurpurea'	0.44 ± 0.009 Cd	0.55 ± 0.009 Be	0.60 ± 0.009 Be	0.78 ± 0.012 Ae
	<i>Ligustrum lucidum</i>	0.25 ± 0.003 Df	0.31 ± 0.003 Cg	0.43 ± 0.003 Bf	0.53 ± 0.009 Ag
	<i>Cornus alba</i>	0.29 ± 0.003 Df	0.36 ± 0.003 Cfg	0.47 ± 0.003 Bf	0.67 ± 0.009 Af
	<i>Syringa oblata</i>	0.92 ± 0.012 Ca	1.15 ± 0.070 BCa	1.31 ± 0.006 Ba	1.58 ± 0.009 Aa
	<i>Forsythia suspense</i>	0.50 ± 0.009 Dc	0.760 ± 0.006 Cd	0.87 ± 0.003 Bd	0.94 ± 0.009 Ad
	<i>Lonicera maackii</i>	0.38 ± 0.012 De	0.80 ± 0.012 Ccd	0.92 ± 0.009 Bc	1.20 ± 0.026 Ac
	<i>Prunus triloba</i>	0.40 ± 0.009 Dde	0.96 ± 0.034 Cb	1.21 ± 0.009 Bb	1.55 ± 0.029 Aa
	<i>Lonicera japonica</i>	0.38 ± 0.009 Ce	0.50 ± 0.009 Bef	0.58 ± 0.019 ABe	0.6 ± 0.003 Ag
	<i>Rosa xanthina</i>	0.27 ± 0.009 Df	0.34 ± 0.006 Cg	0.36 ± 0.011 Bg	0.38 ± 0.012 Ah
	<i>Buxus sinica var. parvifolia</i>	0.60 ± 0.012 Db	0.92 ± 0.012 Cbc	1.24 ± 0.003 Bb	1.44 ± 0.027 Ab
T_g (°C)	<i>Berberis thunbergii</i> 'Atropurpurea'	11.08 ± 0.319 Ad	9.74 ± 0.142 Bf	7.93 ± 0.045 Ce	4.23 ± 0.105 Df
	<i>Ligustrum lucidum</i>	14.20 ± 0.220 Ac	12.56 ± 0.280 Be	10.31 ± 0.048 Cbc	7.28 ± 0.085 Dd
	<i>Cornus alba</i>	14.75 ± 0.313 Abc	13.17 ± 0.263 ABde	11.70 ± 0.2482 Bab	8.19 ± 0.195 Cbcd
	<i>Syringa oblata</i>	15.81 ± 0.217 Aabc	14.72 ± 0.172 Aabc	12.37 ± 0.186 Ba	9.84 ± 0.199 Ca
	<i>Forsythia suspense</i>	14.01 ± 0.194 Ac	13.28 ± 0.283 Ade	11.48 ± 0.260 Bab	8.91 ± 0.067 Cb
	<i>Lonicera maackii</i>	15.50 ± 0.430 Aabc	13.80 ± 0.104 Acde	10.61 ± 0.207 Bbc	8.34 ± 0.175 Cbc
	<i>Prunus triloba</i>	16.78 ± 0.296 Aab	15.14 ± 0.227 Aabc	9.97 ± 0.289 Bcd	7.92 ± 0.192 Ccd
	<i>Lonicera japonica</i>	16.15 ± 0.090 Aa	15.96 ± 0.166 Aa	11.25 ± 0.132 Bab	7.38 ± 0.204 Ccd
	<i>Rosa xanthina</i>	14.11 ± 0.379 Ac	14.17 ± 0.361 Abc	8.93 ± 0.185 Bde	6.09 ± 0.152 Ce
	<i>Buxus sinica var. parvifolia</i>	16.27 ± 0.506 Aab	15.37 ± 0.179 Aab	12.41 ± 0.226 Ba	8.18 ± 0.193 Cbcd
T_a (°C)	<i>Berberis thunbergii</i> 'Atropurpurea'	9.32 ± 0.291 Af	8.52 ± 0.271 fAB	7.10 ± 0.381 Be	2.64 ± 0.225 Ce
	<i>Ligustrum lucidum</i>	12.81 ± 0.208 Ae	11.15 ± 0.173 Be	9.41 ± 0.031 Cbc	4.4 ± 0.144 Dcd
	<i>Cornus alba</i>	13.16 ± 0.148 Ae	12.24 ± 0.242 Ade	10.16 ± 0.212 Bab	5.14 ± 0.081 Cb
	<i>Syringa oblata</i>	14.28 ± 0.147 Ade	11.96 ± 0.205 Bde	11.07 ± 0.204 Ba	6.43 ± 0.278 Ca
	<i>Forsythia suspense</i>	14.72 ± 0.280 Acd	13.77 ± 0.283 Abc	10.03 ± 0.107 Babc	5.65 ± 0.124 Cab
	<i>Lonicera maackii</i>	13.94 ± 0.327 Ade	12.57 ± 0.259 Acd	8.16 ± 0.114 Bd	4.06 ± 0.035 Ccd
	<i>Prunus triloba</i>	17.92 ± 0.290 Aa	15.34 ± 0.189 Ba	9.02 ± 0.194 Ccd	3.20 ± 0.190 De
	<i>Lonicera japonica</i>	16.83 ± 0.334 Aab	15.36 ± 0.079 Ba	9.87 ± 0.046 Cbc	4.66 ± 0.087 Dbcd
	<i>Rosa xanthina</i>	13.32 ± 0.132 Ade	12.47 ± 0.241 Ad	6.78 ± 0.156 Be	3.07 ± 0.060 Ce
	<i>Buxus sinica var. parvifolia</i>	15.83 ± 0.311 Abc	14.2 ± 0.248 Bab	8.28 ± 0.142 Cd	4.29 ± 0.032 Dcd
RH (%)	<i>Berberis thunbergii</i> 'Atropurpurea'	38.58 ± 0.362 Ad	37.11 ± 0.497 Ad	33.91 ± 0.233 Bcd	30.27 ± 0.402 Ce
	<i>Ligustrum lucidum</i>	54.69 ± 0.347 Ab	50.68 ± 0.320 Bb	47.79 ± 0.406 Cb	45.38 ± 0.504 Cb
	<i>Cornus alba</i>	53.87 ± 0.473 Abc	49.35 ± 0.621 Bbc	47.17 ± 0.315 BCb	45.52 ± 0.457 Cb
	<i>Syringa oblata</i>	80.18 ± 0.434 Aa	76.52 ± 0.305 Ba	71.00 ± 0.197 Ca	62.73 ± 0.095 Da
	<i>Forsythia suspense</i>	37.97 ± 0.266 Ade	35.09 ± 0.199 Bde	31.91 ± 0.282 Cef	29.93 ± 0.131 De
	<i>Lonicera maackii</i>	38.74 ± 0.311 Ad	36.70 ± 0.345 Bde	34.91 ± 0.278 BCc	33.04 ± 0.038 Cd
	<i>Prunus triloba</i>	33.58 ± 0.600 Af	29.76 ± 0.187 Bf	31.21 ± 0.116 BCf	28.03 ± 0.148 Cf
	<i>Lonicera japonica</i>	38.23 ± 0.257 Ade	35.65 ± 0.618 ABde	34.27 ± 0.168 Bcd	30.72 ± 0.458 Ce
	<i>Rosa xanthina</i>	51.34 ± 0.587 Ac	47.75 ± 0.273 Bc	47.99 ± 0.245 Bb	42.76 ± 0.123 Cc
	<i>Buxus sinica var. parvifolia</i>	35.97 ± 0.407 Ae	34.63 ± 0.486 ABe	32.82 ± 0.289 Bde	28.18 ± 0.162 Cf
V_v (cmm)	<i>Berberis thunbergii</i> 'Atropurpurea'	52.63 ± 0.315 Da	57.65 ± 0.415 Cd	61.15 ± 0.436 Bd	67.22 ± 0.503 Ac
	<i>Ligustrum lucidum</i>	32.82 ± 0.356 Dde	35.73 ± 0.499 Cf	38.78 ± 0.411 Bg	49.07 ± 0.249 Ae
	<i>Cornus alba</i>	34.11 ± 0.312 Dd	39.23 ± 0.422 Cf	42.81 ± 0.217 Bf	53.75 ± 0.289 Ad
	<i>Syringa oblata</i>	22.37 ± 0.606 Dg	30.43 ± 0.396 Ch	38.60 ± 0.234 Bg	45.49 ± 0.557 Af
	<i>Forsythia suspense</i>	39.12 ± 0.778 Dc	55.43 ± 0.674 Cd	62.12 ± 0.334 Bd	68.08 ± 0.394 Ac
	<i>Lonicera maackii</i>	27.50 ± 0.471 Df	61.50 ± 0.712 Cb	64.85 ± 0.331 Bc	72.16 ± 0.105 Ab
	<i>Prunus triloba</i>	26.82 ± 0.301 Cf	70.88 ± 1.075 Ba	75.01 ± 0.133 ABa	77.46 ± 0.291 Aa
	<i>Lonicera japonica</i>	30.36 ± 0.700 De	42.88 ± 0.418 Ce	46.11 ± 0.105 Be	50.56 ± 0.296 Ae
	<i>Rosa xanthina</i>	20.98 ± 0.267 Db	24.41 ± 0.655 Ci	27.46 ± 0.275 Bh	34.05 ± 0.226 Ag
	<i>Buxus sinica var. parvifolia</i>	42.07 ± 0.410 Dg	66.58 ± 0.754 Cb	71.70 ± 0.158 Bbd	75.97 ± 0.163 Aa

Notes: Values are performed as mean values ± standard errors. The different normal letters in the same column indicate significant differences among treatments at the 0.001 level, while the different capital letters in the same row indicate significant differences among stages at the 0.001 level.

Table A3. Meteorological variables in each measured space (Open green space 3).

		Autumn (White Dew, 09,07)			Autumn (Cold Dew, 10,08)			Winter (Beginning of Winter, 11,07)			Winter (Winter Solstice, 11,07)		
		OGS1	OGS2	OGS3	OGS1	OGS2	OGS3	OGS1	OGS2	OGS3	OGS1	OGS2	OGS3
V_a (m/s)	H	0.45 ± 0.003 d	0.44 ± 0.003 d	0.41 ± 0.009 d	0.61 ± 0.009 c	0.58 ± 0.006 c	0.51 ± 0.009 c	0.76 ± 0.006 b	0.68 ± 0.012 b	0.60 ± 0.138 b	0.82 ± 0.009 a	0.78 ± 0.003 a	0.76 ± 0.012 a
	SH	0.43 ± 0.010 d	0.41 ± 0.06 d	0.35 ± 0.003 d	0.59 ± 0.153 c	0.56 ± 0.06 c	0.50 ± 0.009 c	0.71 ± 0.011 b	0.69 ± 0.06 b	0.66 ± 0.003 b	0.77 ± 0.010 a	0.74 ± 0.009 a	0.71 ± 0.007 a
	AH	0.40 ± 0.003 d	0.37 ± 0.006 d	0.31 ± 0.009 d	0.50 ± 0.009 c	0.47 ± 0.010 c	0.45 ± 0.006 c	0.62 ± 0.011 b	0.61 ± 0.019 b	0.58 ± 0.009 b	0.70 ± 0.009 a	0.68 ± 0.006 a	0.66 ± 0.006 a
	ASH	0.36 ± 0.003 d	0.34 ± 0.003 d	0.23 ± 0.007 c	0.41 ± 0.003 c	0.38 ± 0.006 c	0.39 ± 0.006 b	0.54 ± 0.007 b	0.53 ± 0.003 b	0.53 ± 0.009 a	0.66 ± 0.003 a	0.57 ± 0.003 a	0.57 ± 0.007 a
T_g (°C)	H	9.24 ± 0.118 a	8.39 ± 0.203 a	8.08 ± 0.040 a	7.43 ± 0.082 b	7.36 ± 0.197 a	7.23 ± 0.145 b	5.37 ± 0.116 b	5.20 ± 0.145 c	5.13 ± 0.064 c	4.03 ± 0.088 d	4.03 ± 0.058 c	3.70 ± 0.058 d
	SH	11.40 ± 0.529 a	10.50 ± 0.265 a	10.13 ± 0.188 a	9.83 ± 0.764 a	8.77 ± 0.145 b	8.45 ± 0.232 b	7.43 ± 0.404 b	7.43 ± 0.404 b	7.15 ± 0.736 c	5.73 ± 0.246 c	4.93 ± 0.115 c	4.80 ± 0.058 d
	AH	13.97 ± 0.058 a	13.33 ± 0.203 a	12.40 ± 0.36 a	12.40 ± 0.208 a	11.43 ± 0.379 b	9.69 ± 0.64 b	8.97 ± 0.162 c	8.57 ± 0.296 b	8.15 ± 0.101 c	7.41 ± 0.059 c	6.35 ± 0.174 c	6.08 ± 0.231 d
	ASH	11.43 ± 0.047 a	11.28 ± 0.017 d	11.20 ± 0.103 a	10.31 ± 0.112 b	10.17 ± 0.089 a	10.07 ± 0.033 c	9.54 ± 0.123 b	8.35 ± 0.029 b	8.28 ± 0.041 b	8.17 ± 0.112 c	5.11 ± 0.070 a	4.60 ± 0.750 c
T_a (°C)	H	7.45 ± 0.247 a	7.32 ± 0.072 a	7.06 ± 0.067 a	5.94 ± 0.068 b	5.74 ± 0.029 b	5.11 ± 0.067 b	3.35 ± 0.084 c	2.15 ± 0.077 c	2.03 ± 0.033 c	2.06 ± 0.173 d	1.76 ± 0.031 c	1.55 ± 0.029 d
	SH	8.4 ± 0.100 a	8.38 ± 0.044 a	8.10 ± 0.100 a	7.03 ± 0.033 b	6.45 ± 0.234 b	5.93 ± 0.120 b	4.39 ± 0.194 c	4.03 ± 0.088 c	3.97 ± 0.148 c	3.18 ± 0.356 c	2.10 ± 0.058 d	1.90 ± 0.058 d
	AH	12.10 ± 0.208 a	11.60 ± 0.400 a	10.50 ± 0.289 a	9.73 ± 0.371 b	9.19 ± 0.335 b	7.60 ± 0.306 b	5.23 ± 0.186 c	5.07 ± 0.067 c	4.90 ± 0.100 c	4.47 ± 0.72 c	4.17 ± 0.120 c	4.07 ± 0.115 c
	ASH	11.60 ± 0.400 a	9.92 ± 0.043 a	8.33 ± 0.067 a	9.15 ± 0.074 b	8.50 ± 0.055 a	8.48 ± 0.018 a	6.82 ± 0.064 b	5.78 ± 0.056 b	4.58 ± 0.100 c	5.19 ± 0.241 c	3.18 ± 0.020 d	3.15 ± 0.046 c
RH (%)	H	36.68 ± 0.387 a	35.44 ± 0.281 a	34.85 ± 0.147 a	34.23 ± 0.448 ab	33.60 ± 0.359 a	32.71 ± 0.359 a	31.27 ± 0.410 b	30.82 ± 0.431 b	29.47 ± 0.309 b	25.19 ± 0.478 c	24.52 ± 0.289 c	23.27 ± 0.601 c
	SH	48.56 ± 0.294 a	48.27 ± 0.267 a	38.7 ± 0.153 a	44.90 ± 0.493 b	42.47 ± 0.291 b	37.04 ± 0.166 ab	41.15 ± 0.597 c	39.80 ± 0.115 c	34.71 ± 0.389 b	36.82 ± 0.429 d	35.90 ± 0.493 d	29.04 ± 0.615 c
	AH	52.60 ± 0.529 a	55.27 ± 0.819 a	41.7 ± 0.351 a	49.30 ± 0.351 b	47.60 ± 0.529 b	39.27 ± 0.636 ab	44.97 ± 0.35 bc	42.85 ± 0.790 c	37.17 ± 0.119 bc	40.33 ± 0.882 c	37.5 ± 0.500 d	35.09 ± 0.327 c
	ASH	49.27 ± 0.357 a	49.21 ± 0.116 a	38.82 ± 0.133 a	47.4 ± 0.200 b	45.15 ± 0.076 b	38.26 ± 0.173 b	42.59 ± 0.049 c	41.69 ± 0.164 c	36.76 ± 0.148 b	37.54 ± 0.356 d	37.21 ± 0.107 d	35.00 ± 0.234 c
V_v (cmm)	H	41.90 ± 0.466 d	41.00 ± 0.577 d	40.93 ± 0.468 d	52.16 ± 0.443 c	51.05 ± 0.621 c	48.41 ± 0.747 c	67.74 ± 0.378 b	66.45 ± 0.294 b	57.42 ± 0.550 b	73.53 ± 0.290 a	70.67 ± 0.333 a	67.27 ± 1.124 a
	SH	40.03 ± 0.260 d	39.73 ± 0.187 d	39.00 ± 0.500 d	49.47 ± 0.502 c	48.90 ± 0.587 c	47.59 ± 0.549 c	64.74 ± 0.378 b	64.19 ± 0.424 b	56.49 ± 0.866 b	70.29 ± 0.618 a	69.29 ± 0.633 a	61.34 ± 0.393 a
	AH	38.93 ± 0.515 d	37.50 ± 0.500 d	34.45 ± 0.292 c	50.00 ± 1.155 c	49.00 ± 1.000 c	46.17 ± 0.647 b	60.33 ± 1.155 b	59.67 ± 1.528 b	55.81 ± 0.226 a	68.33 ± 0.333 a	66.33 ± 0.577 a	57.62 ± 0.314 a
	ASH	36.60 ± 0.150 d	34.96 ± 0.031 d	29.18 ± 0.157 d	54.78 ± 0.048 b	46.21 ± 0.107 c	44.56 ± 0.300 c	57.14 ± 0.305 b	54.78 ± 0.048 b	46.45 ± 0.121 b	74.78 ± 0.264 a	66.14 ± 0.071 a	56.75 ± 0.411 a

OGS: Open green space. (a, b, c, d are difference significance analysis, a is significant difference, and so on).

References

1. Kovats, R.S.; Hajat, S. Heat stress and public health: A critical review. *Annu. Rev. Public Health* **2008**, *29*, 41–55. [\[CrossRef\]](#)
2. Chen, H.; Ooka, R.; Kato, S. Study on optimum arrangement of pilotis for design of pleasant outdoor wind environment using CFD simulation and Genetic Algorithms (GA). In Proceedings of the Sixth Asia-Pacific Conference on Wind Engineering (APCWE-VI), Seoul, Republic of Korea; 2005; pp. 1–11.
3. Zellweger, F.; De Frenne, P.; Lenoir, J.; Rocchini, D.; Coomes, D. Advances in Microclimate Ecology Arising from Remote Sensing. *Trends Ecol. Evol.* **2019**, *34*, 327–341. [\[CrossRef\]](#) [\[PubMed\]](#)
4. Li, X.X.; Norford, L.K. Evaluation of cool roof and vegetations in mitigating urban heat island in a tropical city, Singapore. *Urban Clim.* **2016**, *16*, 59–74. [\[CrossRef\]](#)
5. Mushtaha, E.; Shareef, S.; Alsyouf, I.; Mori, T.; Kayed, A.; Abdelrahim, M.; Albannay, S. A study of the impact of major Urban Heat Island factors in a hot climate courtyard: The case of the University of Sharjah, UAE. *Sustain. Cities Soc.* **2021**, *69*, 15. [\[CrossRef\]](#)
6. Zhang, T.; Su, M.; Hong, B.; Wang, C.; Li, K. Interaction of emotional regulation and outdoor thermal perception: A pilot study in a cold region of China. *Build. Environ.* **2021**, *198*, 107870. [\[CrossRef\]](#)
7. Salmond, J.A.; Tadaki, M.; Vardoulakis, S.; Arbuthnott, K.; Coutts, A.; Demuzere, M.; Dirks, K.N.; Heaviside, C.; Lim, S.; Maintyre, H.; et al. Health and climate related ecosystem services provided by street trees in the urban environment. *Environ. Health* **2016**, *15* (Suppl. 1), 36. [\[CrossRef\]](#)
8. Dimoudi, A.; Nikolopoulou, M. Vegetation in the urban environment: Microclimatic analysis and benefits. *Energy Build.* **2003**, *35*, 69–76. [\[CrossRef\]](#)
9. Elwy, I.; Ibrahim, Y.; Fahmy, M.; Mahdy, M. Outdoor microclimatic validation for hybrid simulation workflow in hot arid climates against ENVI-met and field measurements. *Energy Procedia* **2018**, *153*, 29–34. [\[CrossRef\]](#)
10. Bajšanski, I.V.; Milošević, D.D.; Savić, S.M. Evaluation and improvement of outdoor thermal comfort in urban areas on extreme temperature days: Applications of automatic algorithms. *Build. Environ.* **2015**, *94*, 632–643. [\[CrossRef\]](#)
11. Zhang, T.; Hong, B.; Su, X.; Li, Y.; Song, L. Effects of tree seasonal characteristics on thermal-visual perception and thermal comfort. *Build. Environ.* **2022**, *212*, 108793. [\[CrossRef\]](#)
12. Hami, A.; Abdi, B.; Zarehaghi, D.; Maulan, S.B. Assessing the thermal comfort effects of green spaces: A systematic review of methods, parameters, and plants' attributes. *Sustain. Cities Soc.* **2019**, *49*, 11. [\[CrossRef\]](#)
13. Ma, X.; Tian, Y.; Du, M.; Hong, B.; Lin, B. How to design comfortable open spaces for the elderly? Implications of their thermal perceptions in an urban park. *Sci. Total Environ.* **2021**, *768*, 144985. [\[CrossRef\]](#)
14. Yuan, T.; Hong, B.; Qu, H.; Liu, A.; Zheng, Y. Outdoor thermal comfort in urban and rural open spaces: A comparative study in China's cold region. *Urban Clim.* **2023**, *49*, 101501. [\[CrossRef\]](#)
15. Natanian, J.; Kastner, P.; Dogan, T.; Auer, T. From energy performative to livable Mediterranean cities: An annual outdoor thermal comfort and energy balance cross-climatic typological study. *Energy Build.* **2020**, *224*, 18. [\[CrossRef\]](#)
16. Bröde, P.; Jendritzky, G.; Fiala, D.; Havenith, G. The Universal Thermal Climate Index UTCI in operational use. In Proceedings of the Adapting to Change: New Thinking on Comfort, Windsor, UK, 9–11 April 2010.
17. Fang, Y.; Cho, S. Design optimization of building geometry and fenestration for daylighting and energy performance. *Sol. Energy* **2019**, *191*, 7–18. [\[CrossRef\]](#)
18. Ibrahim, Y.; Kershaw, T.; Shepherd, P.; Elwy, I. A parametric optimisation study of urban geometry design to assess outdoor thermal comfort. *Sustain. Cities Soc.* **2021**, *75*, 103352. [\[CrossRef\]](#)
19. Zhang, Q.; Li, X.; Wang, Y. Analysis of climatic characteristics and trends in Lanzhou City during 1981–2016. *Environ. Sci. Pollut. Res.* **2020**, *27*, 32965–32977.
20. Bueno, B.; Norford, L.; Hidalgo, J.; Pigeon, G. The urban weather generator. *J. Build. Perform. Simul.* **2013**, *6*, 269–281. [\[CrossRef\]](#)
21. Bueno, B.; Roth, M.; Norford, L.; Li, R. Computationally efficient prediction of canopy level urban air temperature at the neighbourhood scale. *Urban Clim.* **2014**, *9*, 35–53. [\[CrossRef\]](#)
22. Xu, Y.; Liu, X.; Hu, Y.; Deng, Y.; Li, M. Influence of different tree species on wind environment in urban green spaces: A case study in Guangzhou, China. *Urban For. Urban Green.* **2019**, *38*, 302–310.
23. Shoosharian, S.; Ridley, I. The effect of physical and psychological environments on the users thermal perceptions of educational urban precincts. *Build. Environ.* **2017**, *115*, 182–198. [\[CrossRef\]](#)
24. Galindo, T.; Hermida, M.A. Effects of thermophysiological and non-thermal factors on outdoor thermal perceptions: The Tomebamba Riverbanks case. *Build. Environ.* **2018**, *138*, 235–249. [\[CrossRef\]](#)
25. Yahia, M.W.; Johansson, E.; Thorsson, S.; Lindberg, F.; Rasmussen, M.I. Effect of urban design on microclimate and thermal comfort outdoors in warm-humid Dar es Salaam, Tanzania. *Int. J. Biometeorol.* **2018**, *62*, 373–385. [\[CrossRef\]](#) [\[PubMed\]](#)
26. Sun, T.; Li, X.; Cheng, W.; Zhou, Y.; Wang, M.; Liu, W. Quantifying the impacts of meteorological factors on the urban heat island effect using a spatially explicit network model. *Sci. Total Environ.* **2021**, *753*, 141947.
27. Yang, Z.; Hanna, E.; Callaghan, T.V.; Jonasson, C. How can meteorological observations and microclimate simulations improve understanding of 1913–2010 climate change around Abisko, Swedish Lapland? *Meteorol. Appl.* **2012**, *19*, 454–463. [\[CrossRef\]](#)
28. Piselli, C.; Castaldo, V.L.; Pigliatile, I.; Pisello, A.L.; Cotana, F. Outdoor comfort conditions in urban areas: On citizens' perspective about microclimate mitigation of urban transit areas. *Sustain. Cities Soc.* **2018**, *39*, 16–36. [\[CrossRef\]](#)

29. Burstrom, L.; Bjar, B.; Nilsson, T.; Pettersson, H.; Rodin, I.; Wahlstrom, J. Thermal perception thresholds among workers in a cold climate. *Int. Arch. Occup. Environ. Health* **2017**, *90*, 645–652. [[CrossRef](#)]
30. Jowkar, M.; Rijal, H.B.; Montazami, A.; Brusey, J.; Temeljotov-Salaj, A. The influence of acclimatization, age and gender-related differences on thermal perception in university buildings: Case studies in Scotland and England. *Build. Environ.* **2020**, *179*, 106933. [[CrossRef](#)]
31. Chang, J.; Du, M.; Hong, B.; Qu, H.; Chen, H. Effects of thermal-olfactory interactions on emotional changes in urban outdoor environments. *Build. Environ.* **2023**, *232*, 110049. [[CrossRef](#)]
32. Othman, N.E.; Zaki, S.A.; Rijal, H.B.; Ahmad, N.H.; Razak, A.A. Field study of pedestrians' comfort temperatures under outdoor and semi-outdoor conditions in Malaysian university campuses. *Int. J. Biometeorol.* **2021**, *65*, 453–477. [[CrossRef](#)]
33. Saroglou, T.; Itzhak-Ben-Shalom, H.; Meir, I.A. Pedestrian thermal perception: Studies around two high-rise buildings in the Mediterranean climate. *Build. Res. Inf.* **2021**, *50*, 171–191. [[CrossRef](#)]
34. Peng, Y.; Peng, Z.; Feng, T.; Zhong, C.; Wang, W. Assessing Comfort in Urban Public Spaces: A Structural Equation Model Involving Environmental Attitude and Perception. *Int. J. Environ. Res. Public Health* **2021**, *18*, 17. [[CrossRef](#)] [[PubMed](#)]
35. Ma, X.; Song, L.; Hong, B.; Li, Y.; Li, Y. Relationships between EEG and thermal comfort of elderly adults in outdoor open spaces. *Build. Environ.* **2023**, *235*, 110212. [[CrossRef](#)]
36. Li, Y.; Hong, B.; Wang, Y.; Bai, H.; Chen, H. Assessing heat stress relief measures to enhance outdoor thermal comfort: A field study in China's cold region. *Sustain. Cities Soc.* **2022**, *80*, 103813. [[CrossRef](#)]
37. Crawley, D.B.; Lawrie, L.K.; Winkelmann, F.C.; Buhl, W.F.; Huang, Y.J.; Pedersen, C.O.; Strand, R.K.; Liesen, R.J.; Fisher, D.E.; Witter, M.J.; et al. EnergyPlus: Creating a new-generation building energy simulation program. *Energy Build.* **2001**, *33*, 319–331. [[CrossRef](#)]
38. Evola, G.; Marletta, L.; Cimino, D. Weather data morphing to improve building energy modeling in an urban context. *Math. Model. Eng. Probl.* **2018**, *5*, 211–216. [[CrossRef](#)]

Disclaimer/Publisher's Note: The statements, opinions and data contained in all publications are solely those of the individual author(s) and contributor(s) and not of MDPI and/or the editor(s). MDPI and/or the editor(s) disclaim responsibility for any injury to people or property resulting from any ideas, methods, instructions or products referred to in the content.